Universidade de Lisboa

Faculdade de Farmácia

EVALUATION OF THE MECHANICAL PROPERTIES OF POWDER PARTICLES INTENDED FOR INHALATION

Inês da Conceição Barradas Cachola

Dissertation supervised by Professor Doctor João F. Pinto
and co-supervised by Master of Science Joana T. Pinto

Master Degree in Pharmaceutical Engineering

2018

Universidade de Lisboa

Faculdade de Farmácia

EVALUATION OF THE MECHANICAL PROPERTIES OF POWDER PARTICLES INTENDED FOR INHALATION

Inês da Conceição Barradas Cachola

Dissertation supervised by Professor Doctor João F. Pinto
and co-supervised by Master of Science Joana T. Pinto

Master Degree in Pharmaceutical Engineering

2018

ABSTRACT

Pulmonary drug administration has been the subject of investigation due to its advantages such as the avoidance of the first pass effect, rapid onset of action and small drug doses. Carrier-based dry powder inhalers (DPI) are, as the name indicates, dry powder formulations of inhaled medications. In these, the micronized active pharmaceutical ingredient (API) is blended with coarser excipient particles, the carrier, to provide better bulk properties, flowability and achieve reproducible dosing. However, the production of DPI products is quite complex and to obtain stable formulations, particle properties of the API, excipients and their respective mixtures are important factors to consider. The aim of this work was to understand how the mechanical properties of distinct powder particles intended for inhalation, influence the powder bulk properties and, consequently, their influence in the *in vitro* aerodynamic performance of DPIs. For this, jet-milled Salbutamol Sulphate (SS) was selected as a model API and four different grades of lactose (Duralac© H, Flowlac© 90, Respitose© SV003 and Lactohale© 100) were chosen as potential carriers. Adhesive blends of API (2%) and excipients were produced. Particle size distribution (PSD), hardness, porosity and flowability of the powders and blends were studied. It was found that the API increased the values of tensile strength of pure lactoses due to a decrease in porosity. Also, it was demonstrated that cohesivity and compressibility of the powder bed of the raw materials and blends increased with the presence of a higher percentage of fine particles. However, the latter turned the powders less permeable to air. Finally, the aerodynamic performance of the adhesive blends was tested using a Next Generation Impactor (NGI), at two different flow-rates: 60 and 100 L/min. It turned out that a higher flow-rate resulted in a higher fine particle fraction (FPF) values for all the blends. The best performance was achieved with SS+Duralac© H, being unresponsive to different flow-rates and having the highest and constant values of FPF.

Keywords: Adhesive mixtures; carrier; dry powder inhalers (DPIs); lactose; salbutamol sulphate

RESUMO

A administração de fármacos via pulmonar tem sido objeto de estudo devido às suas vantagens, nomeadamente evitar o efeito de primeira passagem, rápido início de ação e menores concentrações de fármaco necessárias. De facto, o pulmão é um excelente órgão para a distribuição da substância ativa (SA) por todo o corpo, uma vez que tem uma grande área de absorção (~100 m^2), com uma fina membrana de absorção (0.1-0.2 μm) e um fluxo elevado de sangue (5 L/min). Contudo, a administração de fármacos via pulmonar pode ser bastante complexa e, por essa razão, existem vários aspetos a ter em consideração aquando do desenvolvimento de produtos de inalação oral, como por exemplo o tipo de inalador, a sua formulação, bem como as condições físicas do paciente. Este tipo de administração é utilizado, maioritariamente, para o tratamento de doenças do foro respiratório, como por exemplo a asma, doença pulmonar obstrutiva crónica (DPOC) e fibrose quística.

Tal como supracitado, a eficiência da administração de fármacos via pulmonar está altamente dependente do inalador escolhido. Para tal, é necessário ter em conta outros aspetos importantes, como o tipo de SA a ser usada, as suas propriedades físico-químicas, o tipo de formulação e o próprio *design* do inalador que deverá ser compatível com a formulação e adequado à população alvo. Deste modo, o inalador ideal deverá ser fácil de usar, de transportar e o seu desempenho deverá ser o mesmo independentemente das diferentes fisionomias dos pacientes. Existem diversos tipos de dispositivos para este tipo de administração de fármacos, de onde entre eles se destacam os inaladores de pó seco (DPIs), correspondendo, tal como o nome indica, a formulações de pó seco de medicamentos de inalação. Nestes, a SA micronizada é misturada com excipientes de maiores dimensões, denominados de transportadores, de modo a proporcionar maior fluidez e conseguir uma dosagem reprodutível. Não obstante, a produção de DPIs é bastante complexa e para obter uma formulação estável, as propriedades físico-químicas da SA, excipientes e respetivas misturas são fatores importantes a serem considerados, uma vez que estas têm um impacto significativo em todo o processo e no desempenho aerodinâmico da formulação em si. Estas propriedades incluem o estado sólido (dividindo o material em cristalino ou amorfo), micromerítica e a morfologia da superfície das partículas. Além disso, depois da mistura realizada, também se deve proceder a um estudo quanto às interações estabelecidas entre as partículas de SA e as de excipientes, bem como a fluidez da formulação e, por último, o desempenho aerodinâmico.

O objetivo desta tese passou por perceber como as propriedades mecânicas de partículas distintas destinadas a inalação afetam as propriedades do *bulk* e, consequentemente, a sua influência no desempenho aerodinâmico dos DPIs. Para isso, o sulfato de salbutamol (SS) moído a jato foi selecionado como modelo de SA e quatro tipos diferentes de lactose

nomeadamente, Duralac© H, Flowlac© 90, Respitose© SV003 e Lactohale© 100, foram escolhidos como potenciais transportadores a serem utilizados.

Numa fase inicial procedeu-se a um estudo detalhado do SS moído a jato e das quatro lactoses anteriormente citadas, verificando-se que a SA apresenta características que não são benéficas à sua administração via pulmonar por si só, sendo que as suas partículas apesar de pequenas e de se encontrem dentro do intervalo desejável para atingirem os pulmões (1-5 μm), são bastante adesivas, o que as leva a aderirem fortemente umas às outras, formando grandes aglomerados indesejáveis. Ainda, o valor de Span obtido para as matérias primas demonstrou que quanto maior o Span, maior a percentagem de partículas finas presentes na amostra, significando também uma distribuição heterodispersa, o que é positivo para obter uma boa performance aerodinâmica do produto. Ficou também esclarecido que o SS apresenta um maior valor de resistência tênsil e, consequentemente, é a matéria prima menos porosa. Quanto às lactoses estudadas, o Flowlac© 90 é aquela que apresenta maior resistência tênsil, o que está associado à sua forma esférica relacionada a uma menor tendência a deformar/partir, compactando de uma forma mais coesa. De entre as lactoses com uma forma menos regular, o Duralac© H é a lactose que apresenta maior valor de resistência tênsil, pelo que é conclusivo que uma maior percentagem de partículas finas também influencia esta propriedade. Finalmente, a compressibilidade, permeabilidade e coesividade foram examinadas, demonstrando que a SA é a matéria prima que apresenta uma maior compressibilidade e coesividade e, em contraste, uma menor permeabilidade, estando estes resultados associados também à maior quantidade de partículas finas.

Para melhorar algumas das características indesejáveis da SA, foram produzidas misturas adesivas contendo 2% de SS e lactose como excipiente. Antes de proceder à mesma análise realizada para as matérias primas, a homogeneidade das misturas foi testada de forma a garantir que as partículas de excipiente e SA se encontravam bem dispersas. Foi conclusivo que a mistura com maior percentagem de finos era a SS+Duralac© H o que levou a que esta mistura também fosse aquela com maior coesividade e compressibilidade, apesar de tornar as misturas menos permeáveis ao ar. Quanto à resistência tênsil, o SS+Flowlac© 90 é aquela que apresenta um valor superior devido à sua forma mais esférica, tal como já referido anteriormente. No entanto, seria de esperar que esta apresentasse um valor de porosidade inferior, o que não se verificou, provavelmente por alterações decorrentes da compressão do pó.

Finalmente, depois de desenvolver uma nova formulação para DPIs, o seu desempenho aerodinâmico deve ser testado. Este é realizado através de testes *in vitro*, de modo a determinar-se a possível ação *in vivo* da formulação, simulando a deposição do aerossol no pulmão humano. É sabido que existem diversas propriedades que influenciam este teste, tal como a percentagem de partículas finas, permeabilidade e compressibilidade, a forma das

partículas, entre outras. Existem diferentes procedimentos a ser aplicados num teste *in vitro* como este, sendo que os mesmos variam no meio em que as partículas se depositam: os *impingers* usam um meio líquido para a recolha das partículas e os *impactors* recorrem ao meio seco. Neste caso, o desempenho aerodinâmico foi testado recorrendo a um *Next Generation Impactor* (NGI), usando duas taxas de fluxo diferentes: 60 e 100 L/min. As partículas foram, então, fracionadas de acordo com o seu tamanho e a partir daí foi possível determinar o diâmetro aerodinâmico das mesmas, uma vez que os aerossoles são constituídos por partículas de diferentes tamanhos, exibindo diferentes energias, massas e velocidades associadas. Assim, foi possível entender que as partículas com um maior diâmetro aerodinâmico e, consequentemente, as mais pesadas, impactaram ao longo da primeira parte do NGI, uma vez que não se conseguem ajustar rapidamente à mudança de direção do fluxo de ar aplicado, enquanto as partículas mais pequenas impactaram mais tarde. Além disso, verificou-se também que a percentagem de dose emitida do dispositivo de inalação utilizado foi constante independentemente do fluxo de ar utilizado, apresentando um resultado desejado, uma vez que a dose administrada deverá ser sempre constante, independente da capacidade de inalação do paciente. Através deste estudo foi ainda possível concluir que a uma maior taxa de fluxo, as misturas apresentaram uma maior fração de partículas finas (FPF), com exceção para as misturas SS+Duralac© H e SS+Respitose© SV003 cujo valor de FPF continuou praticamente estável. Assim, o melhor desempenho foi alcançado com o SS+Duralac© H, visto que apresentou valores constantes de FPF, dose emitida e não responde, deste modo, às diferentes taxas de fluxo. Foi também possível concluir que existe uma relação positiva entre a percentagem de partículas finas presentes numa formulação e o seu desempenho aerodinâmico.

Palavras-chave: Inalador de pó seco; misturas adesivas; sulfato de salbutamol; transportadores *(carriers)*

ACKNOWLEDGEMENTS

Firstly, I would like to thank to my supervisors Prof. Dr. João F. Pinto and MPharm. Joana Pinto, for the guidance, support and patience throughout these months. Also, I'm really thankful to Dr. Sarah Zellnitz and Dr. Amrit Paudel, for the help and given advices.

Furthermore, thank you to all the chroma and lab team, in special to Paul, for all the funny moments, chocolates and, above all, for being helpful and supportive. Thank you to Feroz and Mike as well, for all the trainings, support and help during my stay in RCPE.

Às minhas melhores amigas, Catarina e Maria, muito obrigada pelas conversas via Skype, pela motivação que me deram ao longo deste período, por ouvirem os meus desabafos e por me fazerem chorar de tanto rir!! Vocês são as melhores!!

Aos grandes amigos que a faculdade me deu: Vera e Tiago! Obrigada pelos ótimos momentos que passamos, passámos e passaremos juntos, bem como pelo apoio neste processo. Tiago, um especial obrigada pela paciência que tiveste em ajudar-me durante a escrita desta tese e pelos teus conselhos; foram essenciais!

Os amigos que fiz em Graz também não podem ficar de fora: Obrigada Rita, Catarina, Cristina, Tiago, Gonçalo, Mariana T. e B., Zé Maria, Pedro, Cátia e Carlos! Thank you, Laura and Joe! Gracias Alvaro! Хвала, Tijana! Teşekkür Ederim, Atay! All the moments we shared were really important for me and you made my stay in Graz unforgettable.

Rita, devo-te um agradecimento especial: obrigada por me "acolheres", por me fazeres rir, pelos passeios, pelas francesinhas, pela Ópera e por tantos outros momentos... Acima de tudo, obrigada por seres tão atenciosa! Vemo-nos em Aveiro (ou em Serpa)!!

Outro gigante agradecimento tem de ir para ti, Cátia! As tuas palavras doces e de apoio, bem como a tua companhia durante os longos dias de trabalho foram essenciais para que eu continuasse motivada e não perdesse o foco no que estava a fazer. Foste como uma irmã mais velha para mim.

Finalmente, gostaria de agradecer ao meu namorado e à melhor família do mundo!

Miguel, não há muito que eu possa dizer que tu não saibas já: obrigada pelo apoio constante e pelos conselhos que me deste, pelas longas chamadas telefónicas e por ouvires os meus desabafos, choros e gargalhadas.

Aos meus tios, primos e avós, obrigada! Um especial agradecimento aos meus avós pelo apoio e amor incondicional, à minha avó pelas gargalhadas que me arranca constantemente e ao meu avô pelos conhecimentos que me transmite desde sempre.

Aos meus pais penso que nunca vou conseguir agradecer o suficiente. Sem vocês, tudo isto teria sido impossível. Obrigada por me encorajarem a seguir os meus sonhos e por apoiarem todas as minhas decisões, mesmo que algumas vezes não sejam as mais corretas. Obrigada por me motivarem todos os dias!

Por fim, ao melhor irmão do universo, o meu: André, obrigada pelas conversas, parvoíces e palhaçadas, por me motivares e me animares durante estes meses, especialmente nas últimas semanas, quando o calor insuportável do Alentejo não dava tréguas e trabalhar não estava a ser nada fácil!

TABLE OF CONTENTS

LIST OF TABLES

LIST OF FIGURES

LIST OF ABBREVIATIONS

API: Active pharmaceutical ingredient
APSD: Aerodynamic particle size distribution
CLF: Coarse lactose fines
COPD: Chronic obstructive pulmonary disease
C_{opt}: Optical concentration
CPS: Percentage by which the bulk density has increased with an applied normal stress (kPa)
DSC: Differential scanning calorimetry
DPI: Dry powder inhaler
DTA: Differential thermal analysis
$Dv_{0.5}$: Mean particle size
ED: Emitted dose
EDD: Emitted dose of the dose
FPD: Fine particle dose
FPF: Fine particle fraction
FTIR: Fourier transform infrared spectroscopy
GSD: Geometric standard distribution
Lβ: Duralac© H
LHα-sph: Flowlac© 90
LHα-tom_lar: Lactohale© 100
LHα-tom_sm: Respitose© SV003
MMAD: Mass median aerodynamic diameter
MOC: Micro-orifice Collector
NGI: Next generation impactor
OIPs: Orally inhaled products
PD: Pressure drop
PDI: Polydispersability
pMDI: Pressurized metered-dose inhaler
PSD: Particle size distribution
RSD: Relative Standard Deviation
SEM: Scanning electron microscopy
SSA: Specific surface area
SSi: Supersonic shear imaging
SWAXS: Small and wide-angle X-ray scattering
SS: Salbutamol Sulphate
TS: Tensile strength
VMD: Volume mean diameters

1. INTRODUCTION

Pulmonary route can be used to deliver drug substances in form of aerosols or vapours into the lungs, for a systemic or local therapeutic effect[1,2]. Through this method of delivery, it is possible to treat respiratory diseases such as asthma, chronic obstructive pulmonary disease (COPD) and cystic fibrosis[1]. When compared with other routes of administration, delivery to the lungs has some significant advantages, such as the reduced risk of systemic adverse side effects, a rapid onset activity, the ability of administering smaller doses locally (compared to the oral or parenteral delivery) and finally the circumvention of the first pass effect, bypassing the metabolism in the liver[1–4]. In fact, due to its large surface area available for absorption (~100 m^2), with a thin absorption membrane (0.1-0.2 μm) and an elevated blood flow (5 L/min), the lungs can also be used to distribute the active pharmaceutical ingredient (API) through the whole body[4]. Notwithstanding, pulmonary administration can be very complex and several aspects should be taken into account when developing new orally inhaled products (OIPs), i.e. the type of inhaler, the dry powder inhaler (DPI) formulation and the patient's physical condition[5]. As a result, understanding the structure and function of the human respiratory tract and its relationship with the product characteristics are key aspects in the development of new inhalation therapies.

1.1. Respiratory Tract

The respiratory tract is divided in two parts, the upper and the lower part. The upper part is formed by the mouth, oropharynx, larynx and glottis and the lower part consists in the trachea, primary bronchi, bronchioles and alveolar ducts ending up in the alveolar sacs (Figure 1). These alveolar sacs contain bundles of alveoli surrounded by blood vessels, between which the unrestricted gas exchange occurs, guaranteeing blood oxygenation[5]. The respiratory system is divided 23 times, forming a branched system and after each bifurcation, two new airways arise, duplicating the airways after each branching. For this reason, after each bifurcation, the cross-sectional area of each subsequent airway decreases and the cross-sectional area of all airways increases, decelerating the airflow and changing the pattern flow from turbulent in the trachea to laminar in the alveoli, reducing the airflow resistance inside the airways[6].

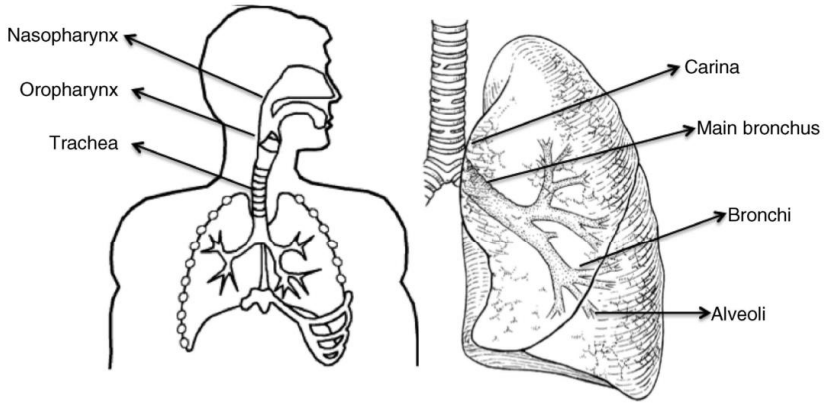

Figure 1 – Schematic representation of the respiratory tract (from [5])

1.2. Deposition of Inhaled Particles

Particles are considered deposited in the respiratory tract when they are definitely removed from the flow streamline. For this reason, it is very important to understand the process and the factors that influence particles settlement in the surface of certain regions of the airway tree. Thus, the deposition of inhaled particles can be determined by the airway geometry, airflow velocity and particle shape. API particle size and its respective distribution are the parameters that are considered more often when engineering particles for pulmonary drug delivery[7]. In order to achieve its therapeutic targets within the lung, it is generally agreed that particles have to be in an aerodynamic size range of 1-5 μm. Particles greater than 5 μm will impact in the throat and do not go into the lungs[8–10].

The aerodynamic diameter of a particle is defined as the diameter of a sphere with a density of ρ=1, that settles in a motionless air with constant velocity as the considered particle (Equation 1):

$$d_{ae} = d \cdot \sqrt{\frac{\rho}{\rho_0 \cdot \chi}} \qquad (1)$$

where d is the diameter of the sphere, ρ is the spherical particle density and ρ_0 is unit density. For non-spherical particles, the particle shape also influences the aerodynamic diameter and, for that reason, a shape factor may also be applied to the equation (χ)[7]. Considering that particles designed for inhalation have often different sizes, the mass median aerodynamic diameter (MMAD) and its geometric standard deviation (GSD) can be used to describe the particle size distribution (PSD). MMAD corresponds to the diameter of a particle where 50% of the total aerosol mass has a smaller particle diameter and the other 50% has a larger particle diameter. The GSD indicates the magnitude of dispersity from the MMAD value[7].

Particle deposition can occur via three different mechanisms: inertial impaction, sedimentation due to gravity and diffusion (Brownian motion)[5,7,8]. When the particles diameter

is larger than 5 µm and as small as 2 µm, inertial impaction is the most relevant mechanism. Particles that deposit through this mechanism are not able to follow the trajectory of the surrounding fluid (air), depositing usually in the upper airways down to the primary bronchi[7,11,12]. Sedimentation is the settling of a particle caused by the force of gravity and its density difference in relation to the surrounding fluid, affect aerosols in the size range of 0.5-5 µm; these particles settle and deposit on the lower surface of an airway[11,12]. At last, particles smaller than 0.5 µm, are mainly deposited due to diffusion. In this case, particles are strongly exposed to collisions with the surrounding gas molecules and exhibit a random movement (Brownian motion). These particles mostly deposit in the alveoli where the velocity of the air is very small[7,11,12].

1.3. Inhalation Devices

The efficiency of pulmonary drug delivery is highly dependent on the device chosen. For the development of an inhaler it is important to take into account several factors, such as the type of drugs used, the physicochemical properties of the drug substance (solubility profile, particle size, morphology and density), the type of formulation (dry powder, propellant driven liquid or aqueous inhalation formulation) and the design of the device for both compatibility with the formulation and suitability for the targeted patient population[13]. A good inhaler, among some other characteristics, should be easy to use, easy to carry and of equal ease of usage in patients with different physical performances[9,14,15].

There are three main types of devices for pulmonary drug delivery: pressurized metered-dose inhalers (pMDIs), nebulizers and DPIs[1,13]. These devices use different approaches to deliver the drug to the lung and they vary in both dosing principle and type of formulation. pMDIs are composed of formulations where the APIs are either dissolved or dispersed in a propellant and, through the actuation by the patient, the liquid phase is nebulized into inhalable particles[16]. In nebulizers, a suspension or an aqueous solution containing API is nebulized, too. However, they are used as stationary devices and hardly ever as portable ones[13]. Finally, as the name indicates, DPIs allow the delivery of a dry powder of the active drug to the lung[9,10].

1.3.1. Dry Powder Inhalers

DPIs are devices made up of three different parts. Each part contributes to the aerodynamic performance and hence to the efficiency of pulmonary drug delivery; namely, these are: the formulation, the dosing/container system and the device with the powder de-agglomeration unit and mouthpiece[8].

There are different categories of DPIs, based in their dose type (Figure 2), i.e.: Single dose, where a capsule or a blister is filled with a metered powder that contains the API and multi

dose, where a formulation is stored in a reservoir container and metered upon activation. In a single-unit dose device, the drug is formulated as a micronized drug powder and carrier system, being inside an individual gelatine capsule, which are is inserted into the inhaler and discarded after use. Concerning the two different multi-dose devices, the multi-dose reservoir stores the formulation in bulk and has a mechanism which allows the inhaler to meter individual doses from the bulk upon inhalation; the multi-unit dose device uses factory metered and sealed doses packaged in a manner that the device can hold multiple doses without having to reload, which is an advantage since the formulation is protected from the environment until use, ensuring adequate control of dose uniformity[17].

These types can be summarized as passive devices or breath-actuated devices, which trigger powder release by the inhalation of the patient. The pulmonary drug delivery with these devices depends on the respirable flow-rate achieved by the patient[9,14,15,18]. On the other hand, there are active DPIs which use integrated facilities such as electrically operated impellors to prompt powder dispersion[16].

The first DPIs on the market were the single dose ones (Figure 3) and these are still in use nowadays. In these, the capsule or blister, which is used just for one application, is pierced by the inhaler device and then, via a deep breath of the patient, the powder is released and delivered into the lungs[16]. An example of a single dose DPI is Pharmachemie *Cyclohaler®*.To overcome the need of refilling the DPI after each use, multi dose DPIs were developed. In these, the powder is filled into an attached reservoir or be contained in multi-unit doses from which metered single doses are administered to the patient[19]. It is important to note that the dose metering system must deliver a consistent amount of the formulation into the airstream. The former depends on the weighing of the container and/or the effective discharge of the compartment during inhalation[20].

The several DPIs can lead to clinically relevant variations in the performance between the different existing devices. Therefore, these must be considered when prescribing a specific device to a certain patient. For example, the inconvenient and complex procedure of loading single-unit dose devices has been associated with a high age related error rate[17].

Recently, *Hovione* launched a single used disposable inhaler which has been accepted worldwide, called *TwinCaps®*. This inhaler can deliver lactose-based or particle-engineered powders and has the capacity to deliver large drug doses. It has been approved in Japan for the delivery of Inavir®, a long-acting neuraminidase inhibitor for the treatment of influenza. *TwinCaps®* has high efficiency, it is a market-leader in Japan and it is entering in USA. Also, it has the lowest number of parts on the market (2 parts) for highest manufacturability in the industry, no metal parts, blades or springs and it is under patent until 2027[21].

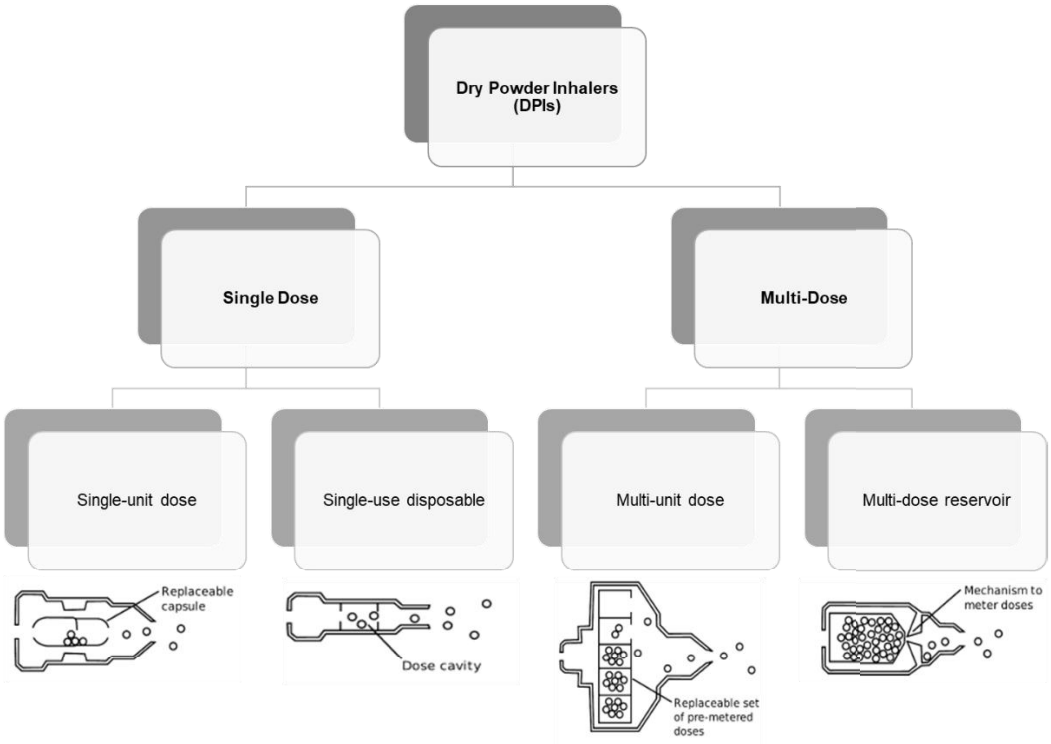

Figure 2 – Types of DPIs and illustrations of four dosing design options available. single-unit dose, single-use disposable, multi-unit dose, multi-dose reservoir (adapted from [17,22])

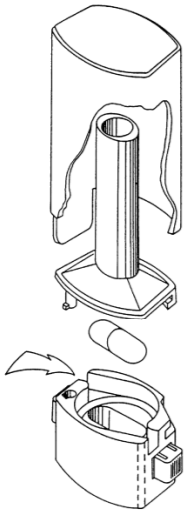

Figure 3 – Capsule-based DPI: one single dose DPI (from [23])

The main difficulty associated with inhalation drug powders and their efficient delivery is the strong interparticle forces which turns the cohesive bulk powder agglomerate. There are three different types of interparticle forces, namely Van der Waals force, which becomes noticeable when particles are close to each other (0.2-1.0 nm) and when particles are small (20 μm or

less), capillary force and electrostatic force. The addition of external energy or reduction of surface force of particles may lower those interparticle forces, since they may alter surface e morphology or surface chemistry. Being that, there are different formulation strategies in DPIs, for example, carrier free, spherical pellets and adhesive mixtures[8,20]. There are some considerable differences between those formulation principles, such as:

Carrier free systems:

- API particles are engineered in a way that allows drug aerosolization without the aid of large excipient particulates;
- Some properties of API particles must be altered and controlled, such as surface roughness (corrugation), particle size, density and shape;
- API particles must be produced using spay drying, super-critical fluid processing and sonocrystallization.

Spherical pellets:

- Spheronized agglomerates of small drug particles which are sieved to obtain easy dispersible pellets with 200-2000 μm;
- More appropriate for high dose drugs (mg range).

Adhesive mixtures:

- Carrier-based formulations, where the fine API particles are mixed with a coarser carrier, which usually is α-lactose monohydrate crystals, since these are approved and generally accepted as safe by most regulatory agencies[8,17,22].

Carrier-based formulations present advantages, such as increasing the bulk of formulation and improving flowability of the small cohesive drug particles. The former allows easier metering of small quantities (usually < 100 μg) of potent drugs improving dosing consistency. The latter improves processing of the formulation (e.g. flow characteristics, avoidance of segregation) during manufacturing and aerosolization during DPI[22].

1.4. DPI Formulation

1.4.1. Particle Engineering

There are several methods to engineer particles. These include spherical crystallization, mechanical milling (jet-milling), spray drying, precipitation and other several techniques[24]. Each of them produces particles with unique physicochemical characteristics that can further affect processing and inhalation performance[8].

The major aim of particle engineering is to improve some characteristics of the powders, taking into account the specifications of the inhaler device that will be used, as well as the intended type of drug delivery[25]. Particles engineered by different methods have different

characteristics. For that reason, solid particles for pulmonary delivery will exhibit different aerosolization behaviours depending on the nature of the interparticulate interactions, type of formulation, inhalation device, flow-rate and breathing pattern[25].

Several techniques have been described in carrier engineering, for example spray-drying, which has been used to produce spherical particles with different surface topographies depending on the process's parameters. Moreover, lactose has been extensively engineered using techniques such as mechanofusion, that results in particles with very smooth surface or spherical crystallization, leading to spherical aggregates of lactose particles[25].

Nowadays, milling is the most common technique to obtain particles between 1-5 μm size range (respirable sizes) and there are several milling methods well established and validated available[26], namely vibration milling, ball milling and jet-milling (fluid energy)[25]. Pressure, friction, attrition, impact or shear lead to the particle size reduction[25]. This process can disrupt the crystalline phase leading to the production of random domains of various molecular disorders, specially amorphous ones[27,28].

Air-jet milling (Figure 4) is the technique used to manufacture inhalation products, which causes particle acceleration, impact, self-attrition, fracture and consequent size reduction[27]. In this technique, particles are carried on a high velocity gas stream (usually with air or nitrogen) into an opposing high velocity gas stream such that particles impinge on each other and the walls of the mill shattering ultimately into respirable sizes. These particles are, then, collected by elutriation[29].

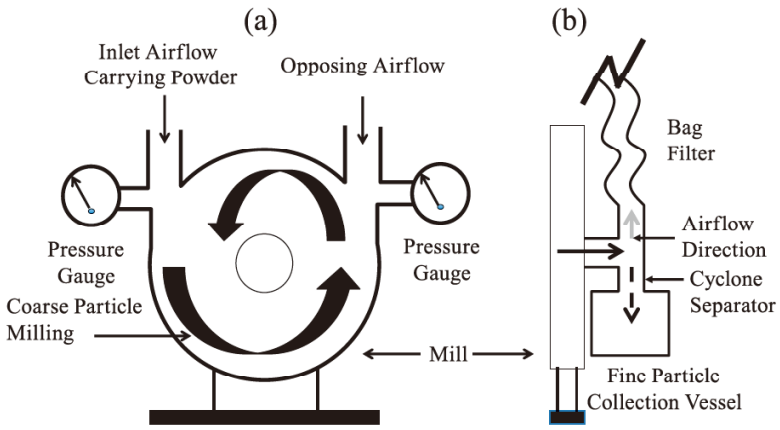

Figure 4 – Schematics of an air-jet mill: (a) front view, showing the opposite high velocity gas stream inside the mill and (b) side view, showing the filter and the collection vessel separated by the cyclone behind the mill

(from [29])

1.4.2. Particle Properties

The physicochemical properties of the carrier and drug may have a strong impact on further processing and on the aerodynamic performance of the formulation. To be able to produce potent adhesive mixtures, it is necessary to analyse and understand the influence of particle properties, since they affect cohesive and adhesive interactions. It is important to say that adhesive forces act between particles with different properties and cohesive forces among particles with similar properties[30]. These properties include solid-state of the material, particle micromeritics and surface morphology[31].

1.4.2.1. Solid-State

To obtain outstanding efficiency of aerosols, it is necessary to develop an optimized formulation and, for that, the solid-state of the powders (chemical and physical stability) must be well known. Usually, the particles can be either crystalline or amorphous[25].

The crystalline form is typically described by polymorphs and pseudopolymorphs. Polymorphism is a phenomenon in which crystals display different lattice structures or molecular conformations without changing its chemical composition. Pseudopolymorphs are crystalline solvates and hydrates, which bound organic solvents or water molecules, respectively, to the crystal structure itself[32]. Amorphous solids usually have a higher dissolution rate and solubility; nevertheless, they present a higher Gibbs free energy, which means they are less stable chemically and physically. For that reason, they can recrystallize, changing the surface characteristics of the powder[33].

During secondary processing (particle engineering), amorphous regions can appear in crystalline materials and this phenomenon called mechanical activation can be beneficial in specific cases and it is usually dominant on the surface[34,35]. Also, reactivity, conductivity, surface free energy and true density are influenced by mechanical activation and these variations might influence the performance of inhalation products[34].

There are several methods to characterize solid-state, such as small and wide-angle X-ray scattering (SWAXS), Fourier transform infrared spectroscopy (FTIR) and differential scanning calorimetry (DSC). In most techniques, the detection limit for quantification of amorphous content is between 5 to 10%, which sometimes can be a problem especially when small amorphous content are on the surface of the powder[36].

1.4.2.2. Micromeritics

Particle Size

Concerning DPI formulations, drug particle size is of extreme importance to assure that drug particles can penetrate the small airways.

According to Kulvanich *et.al*.[37], adhesion forces increase with the decreasing of the particle size. When the size range is below 10 μm, adhesion forces exceed gravitational forces and particles become able to adhere to larger ones. These fine particles are highly sticky, cohesive and have poor flowability because of the dominant attraction force[38]. Thus, it is expected that the API particle detachment during inhalation improves with the decrease of mean drug particle diameter. However, this detachment does not exclusively depends on the attraction forces, but on the magnitude of the removal forces as well and it was observed that increasing the drug particle size enhance particle aerosolization[39]. For this reason, and because the particles of a powder are heterodisperse (different particle sizes are present), it is very important to determine the powder PSD.

The PSD of a powder can be represented by a cumulative or density curve based on number (q0, Q0), length (q1, Q1), area (q2, Q2) or mass/volume (q3, Q3), which can be used to determine a mean particle size ($Dv_{0.5}$) and MMAD[38]. In terms of aerosol quality and efficiency, PSD is a key parameter and is commonly evaluated by the determination of the polydispersibility (PDI), which is usually known as Span value (Equation 2). A higher value of PDI of the carrier indicates a wider PSD, leading to a more heterogeneous blend and can lead to a higher variability in lung deposition of drug upon inhalation[40].

$$PDI = Span = \frac{Dv_{0.9} - Dv_{0.1}}{Dv_{0.5}} \quad (2)$$

Several techniques can be used to measure the PSD, such as sieve analysis, light scattering and laser diffraction, image analysis, etc., the most common one being laser diffraction.

Light-scattering methods (Figure 5) are a commonplace in formulation development[26]. Laser diffraction involves the measurement of a representative sample, dispersed at an adequate concentration in a suitable liquid or gas. For the measurement, the powder should pass through an expanded laser beam. The light of the laser beam is diffracted in different directions, according to the different particle sizes, and the scatter pattern is recorded by detectors. The scatter pattern is related to the particle size and its distribution. The laser diffraction results are often expressed as a volume distribution. The full profile is evaluated, and particle size is generally specified as a three-point specification containing $Dv_{0.1}$, $Dv_{0.5}$ and $Dv_{0.9}$ value. The percentage of fine particles below 5, 10 or 15 μm can also be determined. These parameters can potentially be linked to the product performance[26,41].

The distribution of scattered light is a function of the scattering angle θ, the refractive index of the particle and the dimensionless particle diameter[42], as represented in Equations 3 and 4.

$$I/I_0 = f(\theta, n, \alpha) \quad (3) \qquad \alpha = \frac{\pi d}{\lambda} \quad (4)$$

The algorithms are based on Fraunhofer or Mie theories, from which the particle sizes are determined. Since the algorithms differ among the different instruments, comparison is difficult,

particularly for the majority of pharmaceutical particles, which deviate from sphericity[26]. The theory of Fraunhofer can be used for relatively large particles ($\alpha > 10$) and the theory of Mie can be used for relatively small particles ($0{,}1 < \alpha < 10$)[42].

The scattering pattern of small particles is extremely complex, such that the direct calculation of a particle diameter is impossible. For that reason, calibration with defined particles is used. For a reliable calculation of the particle diameter, multiple detectors are used.

Two examples of laser equipment are *Sympatec* and *Malvern*.

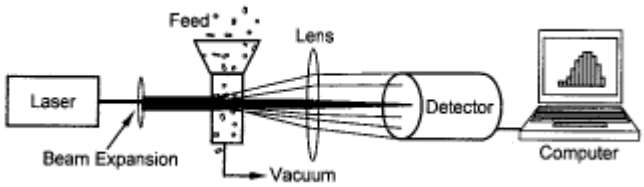

Figure 5 – Schematic representation of a laser-light scattering method, showing how the laser beam passes through the powder and the laser diffract in different directions according to different particle sizes
(from [26])

Also, fine particles have an important role in the aerodynamic performance of DPIs. The definition of "fine particles" is not clear in literature but is defined as particles with a smaller particle size compared to coarse ones. In this thesis, particles smaller than 10 μm were considered "fine particles". Although the numerous studies developed in how fines may affect the performance of DPI formulations, the results are contradictory. Some studies showed that small quantities of fines could increase the deaggregation efficiency and lead to a therapeutical efficacy of the DPI. However, some other studies proved that fines would decrease the deposition of the powder in the lung, decreasing the fine particle fraction (FPF) value[40]. Several theories exist about the role of the fine particles in DPI performance[40,43]:

(a) *Active-sites theory:* active-sites are defined as areas on the carrier surface that are more adhesive than others, which are preferentially occupied by fines. However, there were some criticisms to this idea, since it cannot explain how active sites affect the performance of a powder for inhalation;

(b) *Fluidization theory:* fluidization of a DPI occurs when the pressure drop across the powder bed (PD) is equivalent to the weight of the powder. So, the addition of fines improves DPI performance by increasing the tensile strength (TS) of the formulations, which is related to the interparticulate forces and the free volume of the carrier;

(c) *Agglomeration theory:* the presence of fines results from the formation of drug-fine agglomerates and these are easier to remove from the carrier surface than API particles due to the greater aerodynamic drag force that exists on agglomerates;

(d) *Buffer hypothesis:* usually, commercial α-lactose monohydrate has a rough surface and carries natural fines and impurities on its surface, which may influence their interaction with the drug. Dickhoff *et. al*.[44] developed a study where lactose was submerged in ethanol-water mixtures and it was found that submersion removed the adhering lactose fines, leading to a decrease in drug particle detachment without affecting shape or size of the carrier. Adhering lactose fines act as a buffer between colliding carrier particles and protect smaller drug particles attached to the same crystal planes from the press-on forces that cause increased drug particle detachment during inhalation;

(e) *Case-dependent theory*: Fines do not always improve the aerosol performance of a DPI, which is determined by the formulation and dispersion conditions. According to the study developed by Grasmeijer *et. al*.[45], the presence of coarse lactose fines (CLF) led to a higher detachment of the drug at all flow-rates. To explain these results, two mechanisms are involved: first, fines below a certain size reduce the dispersion performance, increasing the effectiveness of press-on forces; second, lowering TS, CLF may weaken or prevent the formulation of fine particles network.

Particle Shape

The shape of the particle must be considered when developing a DPI formulation. Particle shape is one of the most intractable and uncontrollable factors in powder technology, being important to analyse the influence of this property, since different shapes, such as spherical, tomahawk or irregular, lead to different results. It is known that higher contact areas and shorter interparticulate distances, lead to stronger adhesion forces[38]. Irregular shaped drug particles are usually more cohesive/adhesive than spherical particles[46]. Furthermore, particle shape also has a great impact on the flow behaviour of dispersed particles: elongated particles are very aerodynamic, resulting in a smaller aerodynamic diameter compared to spherical ones, but they tend to have a poorer flowability. Therefore, elongated particles disperse better in a gas stream and penetrate further in a branching system, as is the case of the lungs[38]. On the other hand, spherical particles with low density tend to bind the API for a longer period, reducing the drug loss at different flow-rates and thus enhance the drug delivery[40].

Scanning electron microscopy (SEM) is an example of a method that allows the determination of the shape and morphology of a particle. Also, contact angle measurements (wetting angle using KRÜSS) and optical microscopy are used to determine the particle shape of the powder.

Surface Morphology

Surface area is not exclusively determined by particle size and shape, but also by the morphology of the particle. The morphology of the particle surface determines the contact area

between drug and carrier particles and the magnitude of adhesion forces[38]. Rough particles have more surface area than smooth ones. Thus, particle morphology can also be engineered for DPI formulation design[26,47]. Carrier surface is formed by active sites in which fine drug particles primarily and strongly adhere to. These active sites can have several sources, such as impurities, surface asperities and crystal lattice defects[48]. There is the possibility to create drug particles with specific morphology or select particles to obtain specific surface morphologies and the interparticulate forces can be modulated to enhance lung deposition. Ideally, the contact area and, consequently, the forces should be adjusted to a level that offers enough adhesion between drug and carrier to provide a stable formulation yet allowing easy separation upon inhalation[26].

As mentioned previously, SEM can be used to determine the surface morphology. SEM scans a sample with a focused electron beam over a surface and deliver images with information about the samples' topography and composition (Figure 6)[49]. The electrons interact with atoms present in the sample, which produces signals containing information about the surface topology and composition of the sample. The electron beam is scanned in a raster scan pattern and the position of the beam is combined with the detected signal to produce an image. It is used to study the morphology of the particle, giving information about the roughness or smoothness of the particle itself[50].

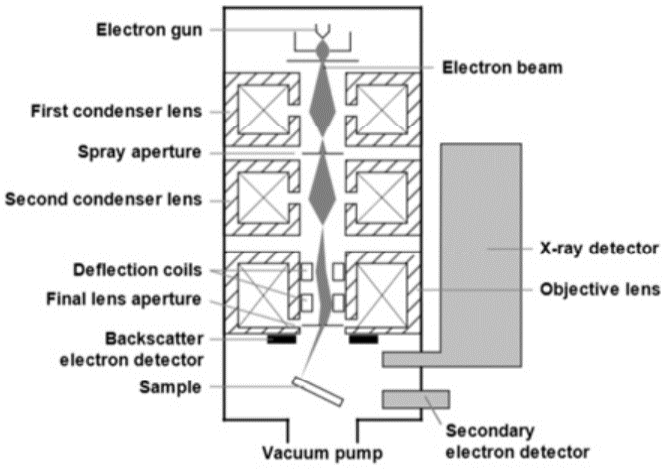

Figure 6 – Schematic representation of the working principle of a scanning electron microscope
(from [51])

1.4.3. Bulk Formulation Properties (Adhesive Mixtures)

It is known that different engineering techniques lead to different solid structures and, consequently, different solid-state behaviours, micromeritics and surface morphologies, influencing particle interaction. The surface energy of a material is the necessary energy to increase the surface area of a solid particle. Therefore, particles with different solid-state

properties, micromeritics and surface morphologies will exhibit different surface energies[38]. For instance, it is known that molecular disordered spots that exhibit higher surface energies can be induced on the surface of the milled particles, resulting in an increased particle cohesiveness and adhesiveness[52]. Drug particles with higher surface energies adhere better to the carrier surfaces[53]. Also, the water uptake of the particles depends on the differences in solid surface structures. When the surface structure is amorphous, the absorption of water is higher, leading to alterations on the particle's morphology, potentially impacting on product performance.

Two different forces act during a mixing process, which are the cohesive forces between the drug particles and adhesive forces between the API and the carrier particles. To complete the mixing process and avoid the agglomeration of the particles, the adhesion force must be high enough. However, the redispersion of the drug affects the performance of the DPI, which is influenced by three factors: the inhaler device, the inhaler manoeuvre of the patient and the formulation. These factors determine the FPF which is the part of the API supposed to reach the deeper part of the lungs[54]. Usually redispersion is easier for smaller carrier particles and the particle surface roughness is a main factor when considering adhesion and friction. In the resuspension process, the particle shape is important for the adhered drug particles, but the shape of the carrier particles might influence the mixing force. During mixing, occurs the friction between the particles of the powder. Friction is smaller for spherical and smooth particles and increases with the increase of the irregularities in the particle shape, increasing interparticle forces. The latter will cause a change in the resuspension properties of the interactive powder mixture[55].

Carrier rugosity and active carrier sites are two important factors for the performance of a DPI. Those can be manipulated by adding fines to the carrier material or other materials[56,57]. Manipulation of the carrier material causes changes in the adhesion forces between carrier and API. The adhesion force should not be too high so that the detachment of the drug particles during inhalation is possible and to avoid the impaction of the API together with the carrier in the upper airways. Thus, the adhesion force is a key parameter for the behaviour of the interactive mixture[54].

1.4.3.1. Flowability

The behaviour of the powder bulk depends on several factors, including the particle properties already mentioned before (particle size, PSD, shape and surface roughness). Besides those factors, flowability, compressibility, dispersibility and fluidization are important to have into account, as well. For example, spherical particles have a higher flowability when compared with irregular particles, due to less interparticle contact points[31,58]. Powder mixtures can be more or less cohesive and this promotes or reduces the aerodynamic performance,

respectively[31]. For this reason, it is important to investigate the behaviour of a powder to draw a conclusion regarding the powder performance during mixing, dosing and aerosolization[31,58]. To analyse the powder bulk, usually a powder rheometer is used, for example, the FT4 equipment (freeman Technology, Tewkesbury, UK).

The powder bulk properties of an adhesive mixture for DPIs depend on the carrier. Poor carrier flowability and low carrier bulk density affects negatively the mixing homogeneity and facilitates segregation[31]. The concentration of the drug at which the powder starts forming particle layers will depend on the interactive capability between the drug particles and carrier and it will influence the bulk of an adhesive mixture. So, if the ratio drug-carrier is high enough, it may result in a multilayer formation of adherent drug particles, even before the carrier surface is covered with a complete monolayer[37]. Also, it is possible that a complete saturation of the carrier surface occurs, resulting in free drug particles (not coupled to the carrier) that agglomerate[59]. Thus, it is advisable that the concentration of drug is adjusted to the physicochemical properties of the carrier, guaranteeing that all drug particles adhere to the carrier surface.

As said before, fine particles are cohesive and have less flowability in contrast to coarse ones. However, it is important that the final formulation has enough flowability to obtain a reproducible dosing during the dispersion from the DPI device. This can be achieved by one of two ways: by controlling the aggregation of particles, forming loosely adherent floccules that improve dispersion or by using carrier-based formulations[60]. The last one has turned out as a challenge, since interactions between the drug and the carrier have an important influence on DPIs performance. Forces acting between carrier and API must be well balanced to guarantee detachment during inhalation.

1.4.3.2. Aerodynamic Performance

After developing a new DPI formulation, *in vitro* aerosolization performance should be tested. These *in vitro* tests allow to determine the possible *in vivo* action of the formulation, simulating the aerosol deposition inside the human lung. Impingers and impactors are two procedures used for testing the *in vitro* performance. The difference between an impinger and an impactor is the medium in which particles deposit: the impingers use liquid impaction plates and impactors use dry ones. However, it is possible to find a similar set-up in both devices; the mouthpiece is fixed on a 90º angled inlet tube, then succeeded by impactor plates (usually four to eight plates) with a filter at the end, where non-deposited particles are collected. There is a vacuum pump that creates an airflow through the plates, as well[61].

There are several types of impactors, but the most used one is the Next Generation Impactor (NGI) (Figure 7). The NGI has a horizontal setup with three main parts: the cut tray, the frame that holds the cup tray and the cover with the fixed nozzles and the inter-stage

pathways. It contains seven impaction stages and a micro-orifice collector that acts as a filter and is responsible for collecting the finest fraction. The air enters the impactor through a bent inlet tube adapted into a pre-separator, where the carrier particles are collected. The air streams zig zags from stage to stage, through nozzle diameters that decrease stepwise and the air velocity increases, leading to a decreasing particle cut-off diameter as impactor stages progress. Each of the stages has a specific cut-off size that can be calibrated[62]. When testing a DPI, the airflow-rate varies between 28 and 100 L/min. Although, it is possible to calculate the cut-off diameters for a specific flow-rate[61] (Equation 5):

$$D_{50Q} = D_{50Qn}\left(\frac{Q_n}{Q}\right)^n \quad (5)$$

where D_{50Qn} is the cut-off diameter of the standardized flow-rate *Qn* (often 60L/min) and D_{50Q} is the cut-off of the applied flow-rate *Q*. The variable *n* depends on the individual stage and varies from 0.54 at stage 1 to 0.67 at stage 7. For this reason, the higher the flow-rate, the smaller the cut-off diameters for the individual stages[61]. To have an adequate correlation between *in vitro* assessment and *in vivo* action of the DPI, the airflow-rate should correspond to a pressure drop of a 4kPa over the device, and a duration consistent with the withdrawal of 4 L of air should be employed[61].

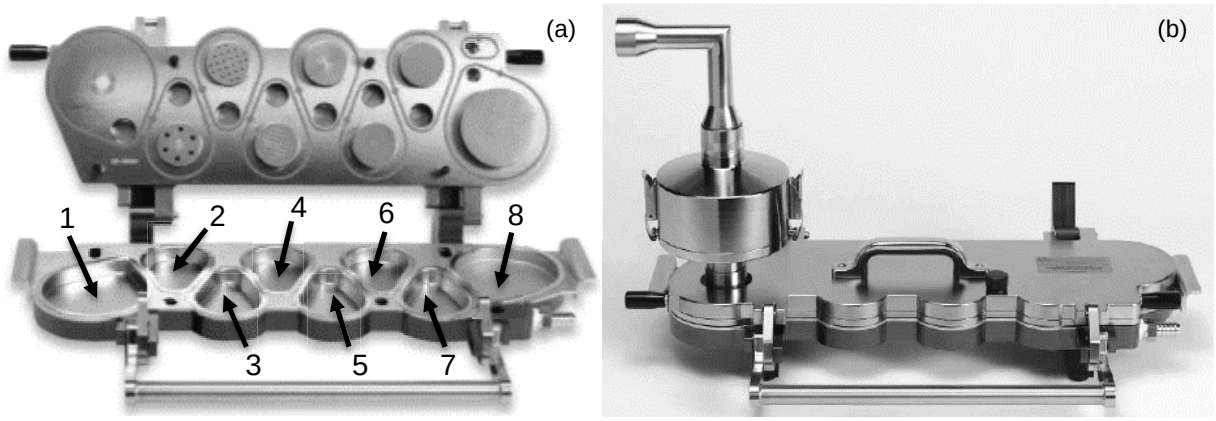

Figure 7 – Representation of the NGI when (a) open, showing the nozzles and collection cups with the indication of the zig zag airstream from stage 1 to 8 and (b) closed, with the 90º bended inlet tube and the pre-separator
(from [62])

DPI formulation *in vitro* assessment is based on inertial impaction of aerosols. Particles get fractionated according to their sizes and from this it is possible to determine the particle aerodynamic diameters. Aerosols are constituted by particles of different sizes that exhibit different energies, particle mass and velocity. Particles with large aerodynamic diameters and heavier ones have a high momentum, so they are not able to adjust fast enough when the air stream changes direction, impacting earlier than small particles that are transported further.

Consequently, the probable impaction of aerosols can be calculated using the particle Stokes number, which is a dimensionless parameter which governs the efficiency of particle impact on a collection plate (Equation 6):

$$Stk = \frac{U_0 \rho d^2 C_c}{9\eta D_n} \quad (6)$$

where U_0 is the average fluid velocity to the nozzle, ρ is the particle density, d is the particle diameter, C_c is the Cunningham slip correction factor, η is the dynamic viscosity of air and D_n is the nozzle diameter. The Cunningham correlation factor is a factor applied to Stokes' law for particles with a diameter of less than 1 μm. This equation assumes that all the particles are spherical, that their Re is less than 0.1 and that their density is greater than air density. The particle will impact on to a plate if its Stokes number is larger than 1[61].

2. AIM OF THE THESIS (HYPOTHESIS)

Particle properties such as PSD, shape and solid-state can influence interparticle interactions that in turn will influence powder bulk properties, i.e. flowability and *in vitro* aerodynamic performance.

Therefore, the aims of this thesis were to understand how the particle properties affect the powder bulk and, consequently, how all these properties influence the aerodynamic performance of carrier-based DPIs and which particle property most influences the aerodynamic performance of carrier-based DPIs. Four different lactoses with distinct solid-state, micromeritics and surface morphologies were chosen to be tested. Jet-milled Salbutamol Sulphate (SS) was used as model API and mixed with the carrier at a load of 2% (wt%). All the raw materials and resulting blends were analysed via PSD by pressure titration, breaking force and powder rheometry. Finally, the aerodynamic performance of the adhesive blends was determined by NGI, obtaining the aerodynamic particle size distribution (APSD) and the FPF.

3. MATERIALS AND METHODS

3.1. Materials

3.1.1. Solvents

Purified water (TKA Wasseraufbereitunssystem GmbH, Germany), acetic acid (Emprove, Merck Millipore, USA) and isopropanol (VWR Chemicals, Germany).

3.1.2. Raw materials: Carriers and API

Micronized SS (Fagron GmbH & Co., Germany) with a particle size of $Dv_{0.1}$ = 0.43±0.01 µm, $Dv_{0.5}$ = 1.53±0.07 µm and $Dv_{0.9}$ = 3.79±0.26 µm was chosen as a model API. Duralac© H (16% α anomer and 83.5% β anomer, Meggle, Germany), α-lactose monohydrate Flowlac© 90 (β anomer ≤ 3%, Meggle, Germany), Respitose© SV003 (β anomer ≤ 3%, DFE pharma, Germany) and Lactohale© 100 (β anomer ≤ 3%, DFE pharma, Germany) were used as model carriers. These powders were chosen as potential carriers due to their distinct solid-states, particle shapes, as well as different values of specific surface area (SSA) (Table 1 and Figure 8).

Table 1 – Characteristics of the potential carriers (Lβ, LHα-sph, LHα-tom_sm and LHα-tom_lar), namely solid-state properties, SSA (m^2/g) and their morphology

Raw material	Sample name	Solid-state	SSA (m^2/g)	Morphology
Duralac© H	Lβ	Anhydrous α- and β-lactose clusters	0.51	Very irregular
Flowlac© 90	LHα-sph	α-lactose monohydrate	0.29	Spherical with irregular surface and deep pores
Respitose© SV003	LHα-tom_sm	α-lactose monohydrate	0.15	Relatively smooth small tomahawk particles
Lactohale© 100	LHα-tom_lar	α-lactose monohydrate	0.13	Relatively smooth large tomahawk particle

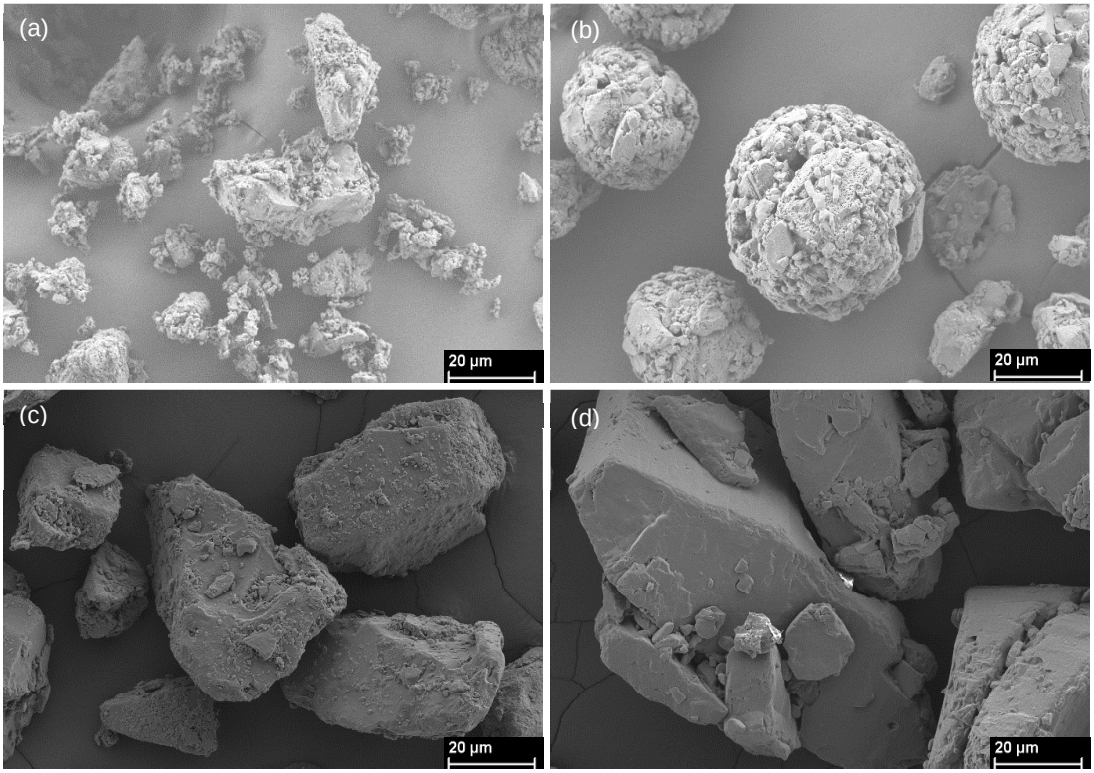

Figure 8 – SEM images of the (a) Lβ; (b) LHα-sph; (c) LHα-tom_sm; (d) LHα-tom_lar (at 228.7 µm width and 500x magnification)

3.2. Preparation and Characterization of the Blends

3.2.1. Preparation of adhesive mixtures

Lactose was dry sieved through sieves (Retsch GmbH, Germany) using a vibratory sieve shaker (Retsch AS200, Germany) to obtain a 20-90 µm particle size fraction.

Adhesive mixtures of 2% jet-milled SS were prepared. 49 g of lactose and 1 g of API were weighed into a vessel using the "*sandwich method*": the first 24 g of the carrier was weighed in the vessel followed by a layer of 1 g of the API and then the rest of the carrier was added. The vessels were blended in a Turbula blender TC2 (Willy A. Bachofen Maschinenfabrik, Muttenz, Switzerland) for 90 min at 62 rpm (criteria stablished based on [27,63]). 4 blends were prepared, one for each lactose studied.

3.2.2. Mixing Homogeneity

Homogeneity of each mixture was determined by taking 10 samples of approximately 25 mg and dissolved in 10 ml of purified water. Samples were taken from the top, centre, bottom and close to the walls of the vessel, ensuring the uniform sampling. For the analysis of the dissolved samples, the absorbance (λ=276 nm) was measured using the UV-VIS

spectrophotometer UV-2700 (Shimadzu, Kyoto, Japan). The measurements were made in triplicate (n=3).

3.3. Powder Characterization

3.3.1. Particle Size Distribution

PSD was evaluated using laser diffraction (HELOS/KR, Sympatec GmbH, Germany). The powder was placed on a vibrating chute (Vibri, Sympatec GmbH, Germany) and dispersed using a dry dispersing system (RODOS, Sympatec GmbH, Germany). A sampling time of 10 s (12 s real time) was applied and measurement with an R2 (0.45-87.5 µm) and R5 lens (4.5-875 µm), triggered once an optical concentration (C_{opt}) of 0.5% was reached. To evaluate the pressure at which the particles de-agglomerate, a pressure titration was applied. For this, the primary dispersion pressure was manually adjusted in 0.2 bar step in the range of 0.1-2.0 bar. Measurements were done in triplicate (n=3) at 0.1, 1.5 and 2.0 bar. Before each measurement, the dispersing system was cleaned using sand and a reference measurement was taken.

Moreover, and in order to evaluate the un-agglomerate state of the samples, the powders were evaluated using wet-dispersion (CUVETTE, Sympatec GmbH, Germany). Isopropanol was chosen as the dispersant medium. 50 ml of the alcohol were added into a stationary cuvette and very small amounts of powder were added, step-wise to the solvent. The system was magnetic stirred (1000 rpm) in order to disperse the samples. Measurements were carried during 120 s, once a C_{opt} above 0.5% was reached.

Particle size cumulative volume and number distribution (cumulative (Q3) and density (q3) distribution and Q0/q0, respectively) were calculated and analysed using Windox 5 software (Sympatec GmbH, Germany).

3.3.2. Hardness and Tensile Strength

The hardness of the plugs of lactose, SS and blends were evaluated using a 3-in-1 hardness, diameter and thickness testing instrument (PTB 311E, PharmaTest GmbH, Germany). For that, it was necessary to compress the powders with a hydraulic press, using a 500 kg load. Measurements were done in quintupled (n=5) and the thickness of the plugs were 3.694±0.269mm. The plug is put on the surface of the testing instrument and the pressure is applied in the lateral area of the plug itself, as represented in Figure 9.

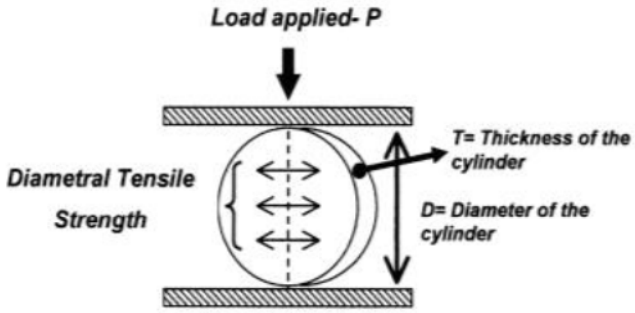

Figure 9 – Schematic representation of the equatorial tablet tensile strength test (From [64])

The TS was calculated using the Equation 7[64]:

$$Tensile\ Strength = 2 \times \frac{Failure\ load\ (N)}{\pi DT\ (m^2)} \quad (7)$$

where *D* is the diameter of the plug and *T* is the thickness of the plug.

3.3.3. Density and Porosity

The density of the materials was tested using a gas pycnometer (AccuPyc II 1340 TEC, Micromeritrics). For this, it was necessary to compress the powders using a hydraulic press. In order to be used, the pycnometer had to be calibrated using three metal spheres and, for the actual measurement, five plugs were placed inside of its chamber. The equipment gives five values of volume that are used to calculate the density of the materials. Knowing the grain density of the plug and the bulk density, it was possible to calculate the porosity using the following formula (Equation 8)[65]:

$$Porosity = 1 - \frac{Bulk\ Density\ (g/cm^3)}{Grain\ Density\ of\ the\ plug\ (g/cm^3)} \times 100 \quad (8)$$

The values of the bulk density, which corresponds to the calculated density, were obtained dividing their mass (g) for the respective volume (cm^3). The grain density of the plugs was directly obtained through the pycnometer.

3.3.4. Dynamic Powder Flow Analysis

To measure the flow properties of the samples, a FT4 Powder Rheometer (Freeman Technology, Welland, UK) was used.

To measure the compressibility, a sample of powder was analysed using a 25 mm bore borosilicate glass cylinder. The samples were conditioned using a 23.5 mm blade which was moved down a helical path, allowing the displacement of the powder, which removes the packing history of the powder and any operator influence and, therefore, generates a homogenized uniform low packing stress in the powder. The cell was then split to remove any

surplus powder. Formerly, the blade was replaced by a piston and a varying normal stress between 1 and 15 kPa was applied on the sample, obtaining eight values of compressibility at different pressures. Measurements were performed in triplicate (n=3).

Powder permeability was measured using a 25 mm bore borosilicate glass cylinder. The samples were conditioned using a 23.5 mm blade which was moved down a helical path, displacing the powder. After conditioning the powder, the cell is split to remove any excess of powder. Permeability studies were conducted at a constant airflow velocity of $2mm.s^{-1}$, which was passed through the powder bed, with varying normal stress between 1 to 15 kPa being applied on to the sample, using a piston. Measurements were performed in triplicate (n=3).

Powder cohesivity was analysed using a 25 mm bore borosilicate glass cylinder. Once again, the samples were conditioned using a 23.5 mm blade which was moved down a helical path, allowing the displacement of the powder. Then, the blade was replaced by a piston which compacted the sample. The cell was split to remove any surplus powder. At that point, the piston was substituted by a 24 mm sear cell and the test was carried out varying normal stress between 5 to 15 kPa being applied on the sample. Measurements were performed in triplicate (n=3).

3.4. Aerosolization Assessment

The aerosolization performance of the blends at both capsule fill settings was determined with a NGI (Copley Scientific, Nottingham, United Kingdom) and according to the procedure described in the US pharmacopoeia (Preparations for inhalation: aerodynamic assessment of fine particles, Ph. Eur., 7.0) and taken from the literature[61]. For the experiments, capsules were filled with, approximately, 40 mg of sample. At first, the vacuum pump (SCP5, Copley Scientific) was switched on and the small trays and the large cups were coated with a coating agent (2% solution of Tween 20 in absolute ethanol). The small impaction trays were coated with 2 ml and the two larger ones with 4 ml of the coating agent and 30 min were waited to guarantee that the coating agent was able to cure completely. The pre-separator was filled with 10 ml of acetic acid buffer (pH=3) and the flow-rate through the device was set to 60 and 100 L/min using a critical flow controller (TPK, Copley Scientific), which was checked with a flow meter (DFM3, Copley Scientific). As an inhalation device, a unit dose DPI was selected: Cyclohaler®.

4. RESULTS AND DISCUSSION

4.1. Particle Characterization of the Raw Materials and Blends

To understand how the particle properties affect the powder bulk and, consequently, how all these properties influence the aerodynamic performance of carrier-based DPIs, some studies were conducted, such as PSD, hardness and porosity, compressibility, permeability and cohesivity. It is known that these parameters have a relationship between them and it was desirable to confirm these relations. However, the main goal of these analysis was to find out how they influence the aerodynamic performance of DPIs and, for that, an NGI analysis was made, which allowed to find which property most contribute to a better performance and, afterward, which lactose had the best characteristics to be an ideal carrier to be used in a DPI formulation.

4.1.1. Blend Homogeneity

To proceed with the study, it was necessary to analyse the mixing homogeneity, as described in section 3.2.2. According to US Pharmacopeia, blends are considered homogeneous when the relative standard deviation (RSD) is less than 5%.

As represented in Table 2, all mixtures are considered homogeneous and, for that reason, the powder properties of the blends could be analysed. Since RSD are below 5%, it was possible to proceed with the research.

Table 2 **–** API content present in the blends and mixing homogeneity, in percentage, for SS+Lβ, SS+LHα-sph, SS+LHα-tom_sm and SS+LHα-tom_lar

Specification	API content (wt%)	Mixing Homogeneity – RSD (%)
SS + Lβ	2.00	2.30
SS + LHα-sph	2.19	2.95
SS + LHα-tom_sm	2.20	3.84
SS + LHα-tom_lar	2.00	3.66

4.1.2. Particle Size Distribution

The laser diffraction system using wet and dry pressure titration was used to identify the presence or not of agglomerates and the respective force necessary to break them. Moreover, the PSD of the different materials was analysed and compared among each other using the volume distribution percentiles, i.e. $Dv_{0.1}$, $Dv_{0.5}$ and $Dv_{0.9}$. Furthermore, the percentage of particles below 10 µm, considering the content of fine particles, was also evaluated.

First, a dry dispersion measurement was performed. This type of measurement permits to overcome the binding forces between agglomerated particles, resulting in the optical dilution of the particle agglomerates, making them measurable by the sensor as individual specimens.

The PSD values obtained at the primary pressures in the range from 0.1 bar to 2.0 bar are presented in Figure 10 and 11 for raw materials and blends, respectively. The particle diameters and Span values are in Table 3 and 4, which allows to understand if the raw material powders and respective blends were mono- or heterodisperse[66].

Table 3 – Particle size volume distribution and respective Span of the jet-milled SS, Lβ, LHα-sph, LHα-tom_sm and LHα-tom_lar at primary dispersion pressure of 0.1, 1.5 and 2.0 bar

Raw Material	$Dv_{0.1}$ (µm)	$Dv_{0.5}$ (µm)	$Dv_{0.9}$ (µm)	Span*
0.1 bar				
Lβ	13.73±4.47	55.41±8.19	105.38±8.31	1.68±0.24
LHα-sph	44.38±2.86	71.95±3.26	108.00±9.11	0.88±0.05
LHα-tom_sm	34.61±1.28	64.29±2.42	110.72±9.81	1.18±0.09
LHα-tom_lar	67.33±2.12	132.95±2.32	216.13±5.46	1.12±0.02
SS	0.68±0.04	3.67±0.46	27.42±24.77	6.83±5.52
1.5 bar				
Lβ	6.57±0.85	53.89±7.94	108.88±5.76	1.92±0.22
LHα-sph	44.07±3.72	73.44±2.96	123.49±16.19	1.08±0.15
LHα-tom_sm	31.51±0.11	63.82±0.21	110.85±1.90	1.24±0.02
LHα-tom_lar	59.71±0.14	131.00±1.32	215.92±4.69	1.19±0.03
SS	0.44±0.01	1.61±0.03	3.97±0.06	2.19±0.05
2.0 bar				
Lβ	6.51±0.80	53.57±7.10	109.00±6.67	1.93±0.16
LHα-sph	44.45±2.93	72.21±0.91	108.53±5.06	0.89±0.10
LHα-tom_sm	30.90±0.07	63.61±0.09	111.74±0.57	1.27±0.01
LHα-tom_lar	58.79±0.79	129.11±1.53	215.68±7.05	1.21±0.04
SS	0.43±0.01	1.53±0.07	3.79±0.26	2.19±0.08

$$*Span = \frac{Dv_{0.9} - Dv_{0.1}}{Dv_{0.5}} \quad (9)$$

Triplicates were carried out (Mean±SD)

Table 4 – Particle size volume distribution and respective Span of the SS+Lβ, SS+LHα-sph, SS+LHα-tom_sm and SS+LHα-tom_lar at primary dispersion pressure of 0.1, 1.5 and 2.0 bar

Raw Material	$Dv_{0.1}$ (µm)	$Dv_{0.5}$ (µm)	$Dv_{0.9}$ (µm)	Span
0.1 bar				
SS+Lβ	6.44±0.36	38.39±6.36	94.18±22.79	2.27±0.24
SS+LHα-sph	35.12±0.32	64.99±0.40	105.17±3.35	1.08±0.04
SS+LHα-tom_sm	32.69±0.58	65.13±1.55	116.87±13.62	1.29±0.18
SS+LHα-tom_lar	60.59±1.19	130.49±1.49	217.50±5.05	1.20±0.02
1.5 bar				
SS+Lβ	3.10±0.18	42.08±1.44	99.78±3.58	2.30±0.03
SS+LHα-sph	28.17±0.74	63.03±0.65	105.04±2.95	1.22±0.02
SS+LHα-tom_sm	15.52±1.13	61.71±0.88	108.49±4.50	1.51±0.04
SS+LHα-tom_lar	31.69±2.72	123.08±1.72	207.98±2.01	1.43±0.03
2.0 bar				
SS+Lβ	2.84±0.23	41.61±2.36	98.85±4.97	2.30±0.02
SS+LHα-sph	26.97±0.55	62.86±0.10	104.01±1.64	1.23±0.02
SS+LHα-tom_sm	14.35±0.90	61.88±0.09	110.14±1.42	1.55±0.02
SS+LHα-tom_lar	28.68±1.02	120.37±1.04	204.91±2.45	1.46±0.00

Triplicates were carried out (Mean±SD)

By comparison of the mean particle size and its Span, it was possible to verify that Lβ is the lactose with larger distribution of particles, since it has the highest value of Span among the lactoses (Table 3). It is also visible that LHα-sph has the lowest value of Span, which means it has a smaller distribution of particles. Moreover, in every primary pressure used, SS particles exhibit a $Dv_{0.5}$ below 5 µm and a higher value of Span, which means that SS had the largest distribution of particles.

Concerning the blends (Table 4), it was possible to verify that SS+Lβ is the blend with larger distribution of particles, since it had the highest value of Span, which was concordant with the result obtained for the raw materials. SS+LHα-sph had the lowest value of Span, having the smaller distribution of particles. Also, in general, it was possible to see that there was a decrease of the values of $Dv_{0.1}$, $Dv_{0.5}$ and $Dv_{0.9}$ when compared with the raw material results, leading to higher values of Span, which is a natural consequence of adding 2% of fine SS particles to the raw coarser carriers.

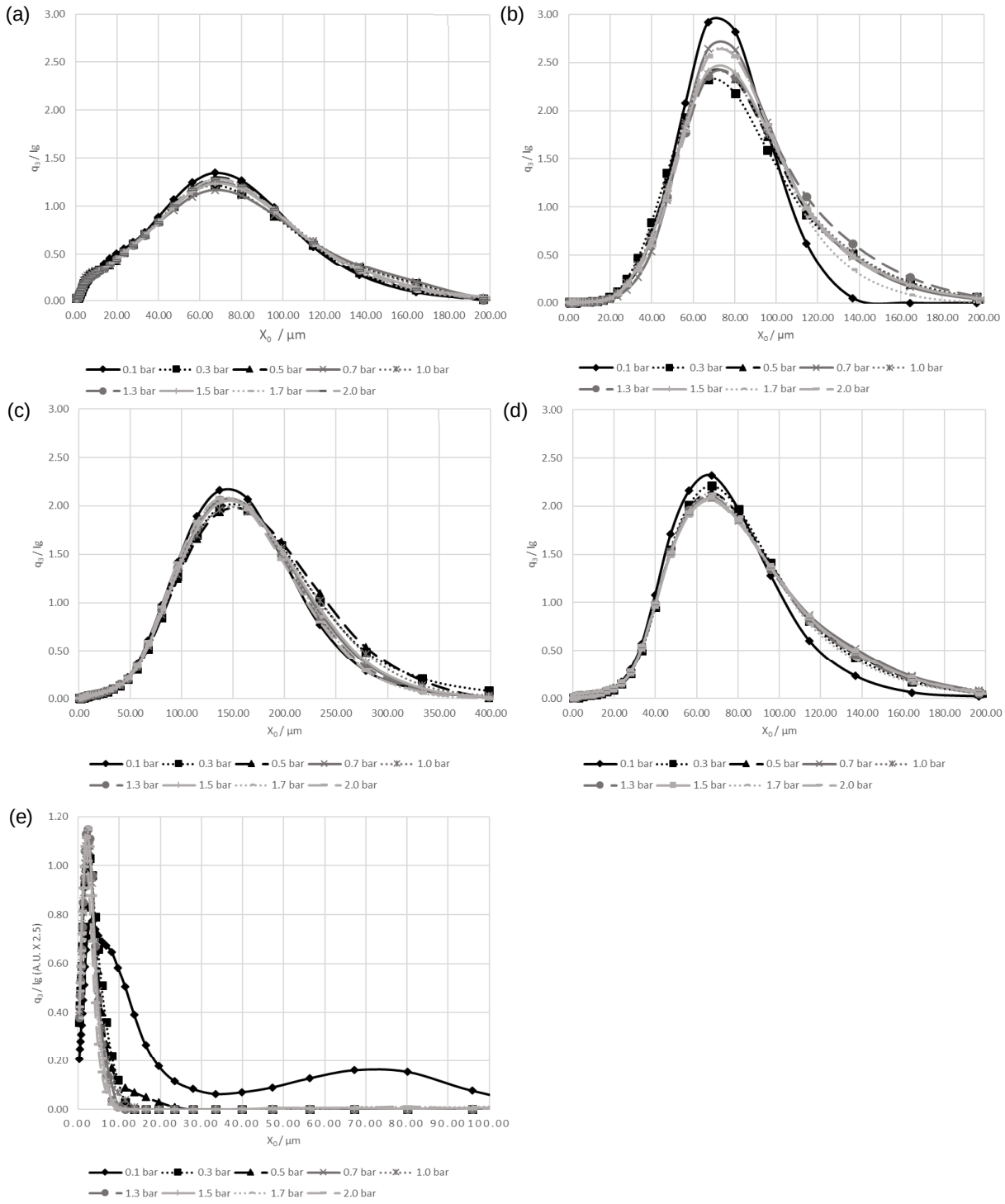

Figure 10 – Particle size density volume distribution at different pressure titrations from 0.1 to 2.0 bar for (a) Lβ, (b) LHα-sph, (c) LHα-tom_sm, (d) LHα-tom_lar and (e) SS Triplicates were carried out at 0.1, 1.5 and 2.0 bar (Mean±SD)

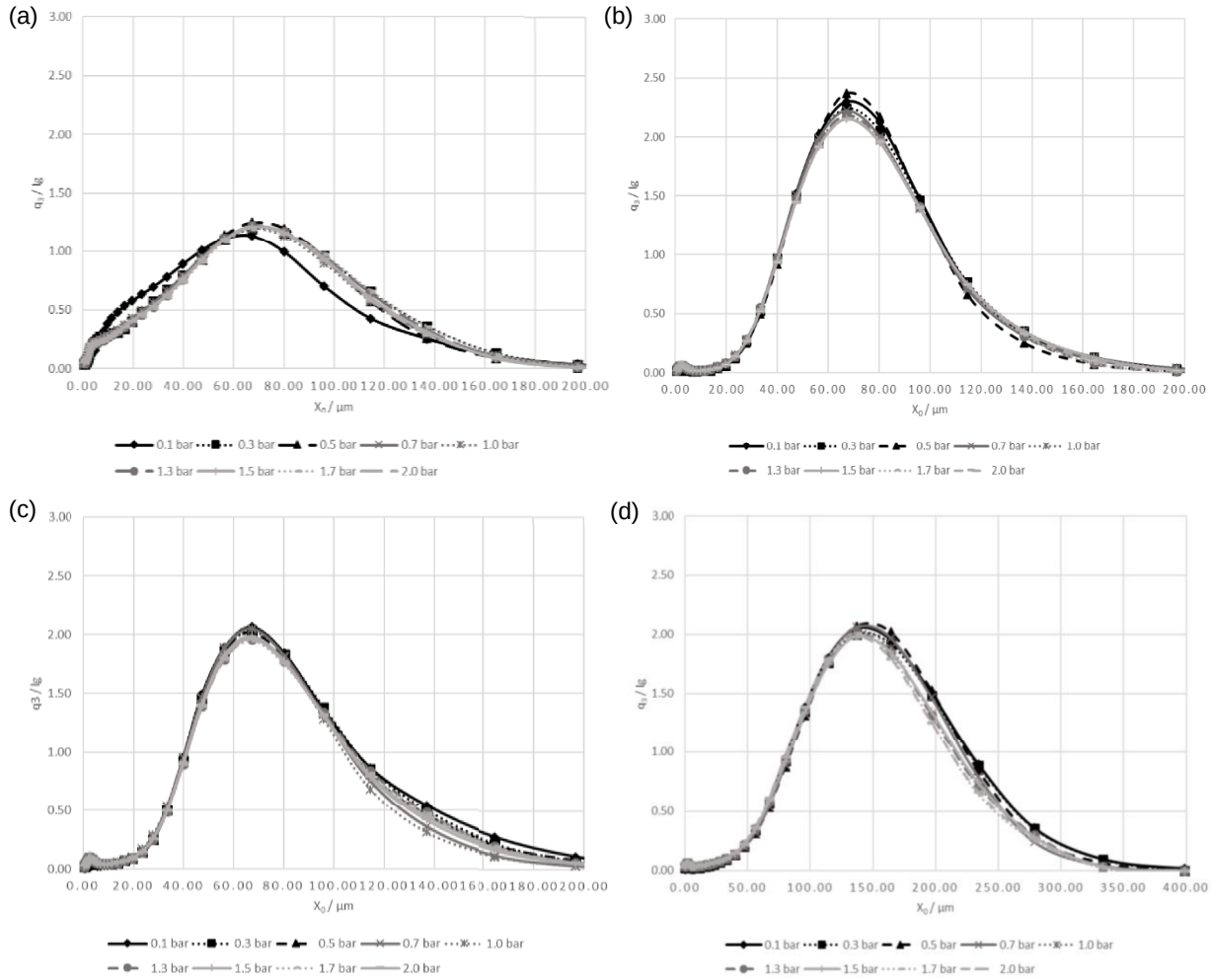

Figure 11 – Particle size density volume distribution at different pressure titrations from 0.1 to 2.0 bar for (a) SS+Lβ, (b) SS+LHα-sph, (c) SS+LHα-tom_sm, (d) SS+LHα-tom_lar
Triplicates were carried out at 0.1, 1.5 and 2.0 bar (Mean±SD)

According to the density distribution represented in Figure 10, Lβ, LHα-sph and LHα-tom_sm have a mean particle size in the range of 65 to 70 µm. However, analysis of Lβ PSD reveals that this carrier has a notable presence of particles smaller than 20 µm, having the smaller mean particle size of all the analysed carriers ($Dv_{0.5}$ = 47.67±4.81 µm, on average). Naturally, LHα-tom_lar presenting the largest particles, have a higher value of $Dv_{0.5}$ ($Dv_{0.5}$ = 132.44±2.90 µm, on average). As described in literature, α-lactose monohydrate has been employed as a carrier in adhesive blends and depending on the design of the DPI device, a mean particle size between 50 and 200 µm[67] is deemed as adequate, being also described that lactose carriers should be one order of magnitude greater than the drug particles (> 50 µm)[68]. Analysing the results in Figure 10 and Table 3, it is seen that Lβ, LHα-sph and LHα-tom_sm are within the mentioned range. Moreover, there are studies using capsule based DPIs that indicate that decreasing carrier particle size can lead to a better aerodynamic performance: studies that used polystyrene spheres with 82.8, 277.5 and 582.9 µm, has

showed exactly that. This result was attributed to the decreasing particle size, including decreased number of drug particles per carrier and the increase in particle number, surface area, intercarrier adhesion and number of collisions in the powder bed during aerosolization[40,68].

Regarding SS, it was apparent that at 0.1 bar the particles were agglomerated, which explains the high percentage of particles found at 70 µm (Figure 10(e)). However, when the dispersion pressure was increased to 0.3 bar, the $Dv_{0.5}$ found was 1.85±0.00 µm and no more particles were possible to be detected at about 70 µm. Moreover, when the pressure was further increased, this resulted in a plateau in the PSD, indicating that no more agglomerates were present. So, it is possible to say that primary particle size of the API was 1.69±0.12 µm, which confirmed that the particles were appropriate to be delivered to the lungs[8–10,27].

Concerning the blends (Figure 11), SS+Lβ, SS+LHα-sph and SS+LHα-tom_sm have a $Dv_{0.5}$ in the range of 65 to 70 µm, the same range encountered for the raw materials. Nevertheless, when a detailed analysis is done, all these blends have now a notable presence of particles smaller than 20 µm, specially SS+Lβ. For this reason, SS+Lβ has the smallest $Dv_{0.5}$ of all the blends (41.97±1.55 µm, on average) and all the other blends have a lower mean particle size when compared with the lactoses by themselves. This, as mentioned before, is happening because the lactoses were mixed with SS, which has a mean particle size of 1.69±0.12 µm. SS+LHα-tom_lar presented the largest particles, having a $Dv_{0.5}$=125.13±3.94 µm, on average, which is, of course, lower than the $Dv_{0.5}$ of the raw material.

Comparing the Span values obtained and the density distribution, it was conclusive that all the raw materials and blends have a heterodisperse distribution. Still, when analysing the blends, it is possible to detect a wider PSD, which is a consequence of a higher percentage of smaller particles present in the mixture[67]. Furthermore, it was seen that raw materials and blends presented a PSD between 2-200 µm, which is in accordance with the targeted gap to obtain a good DPI performance[68].

An important parameter to consider in the formulation of carrier-based DPIs is the percentage of fines within the blend (described in section 1.4.2.2.1). In this work, “fines” were considered all the particles in the sample which were smaller than 10 µm. In Figure 12 are represented the distribution of the percentage of fine particles found in carriers, API and blends.

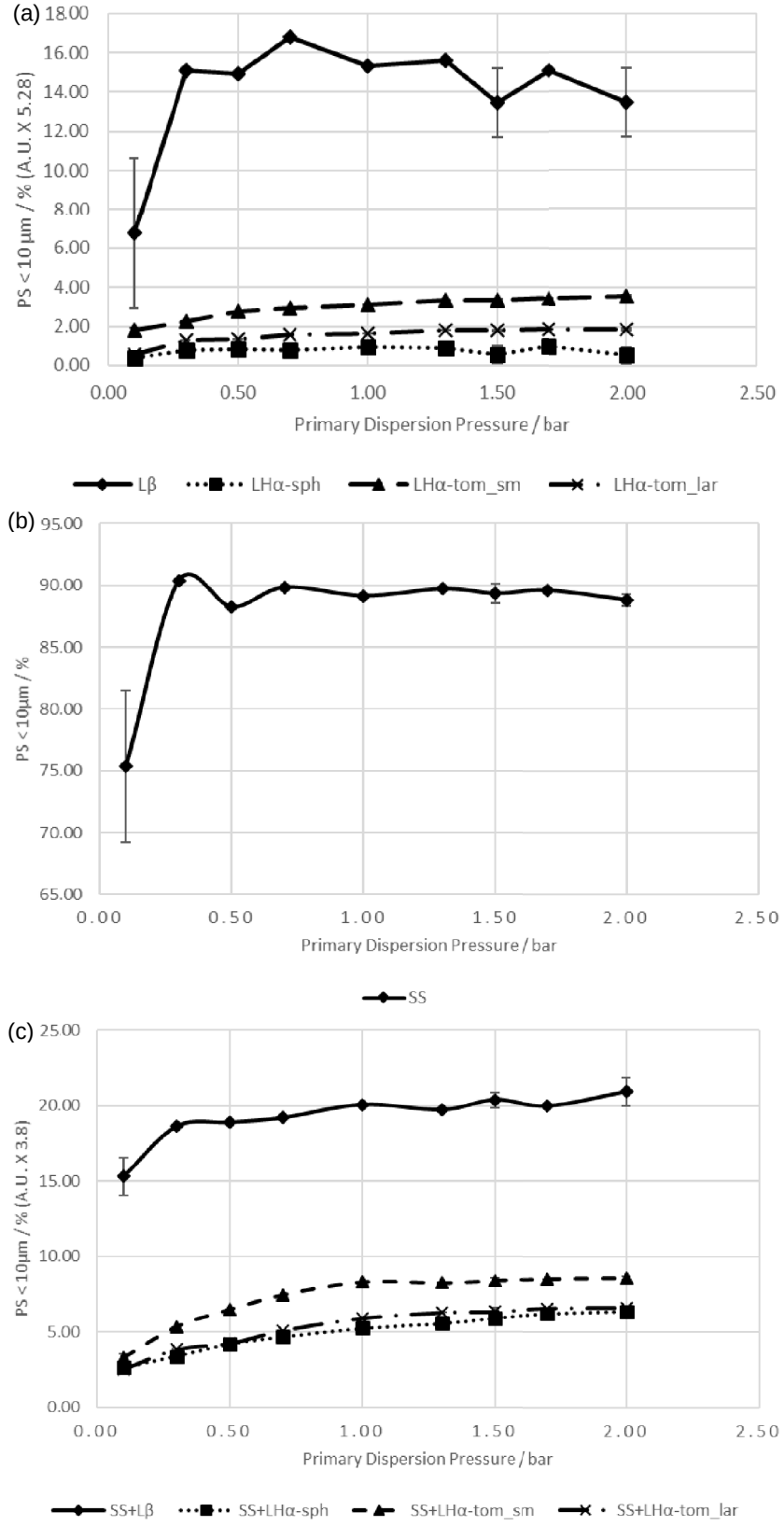

Figure 12 – Percentage of fine particles (smaller than 10 µm) present in the samples at different pressure titrations from 0.1 to 2.0 bar for (a) carriers, (b) API and (c) blends Triplicates were carried out at 0.1, 1.5 and 2.0 bar (Mean±SD)

Figure 12(a) confirms that Lβ is the lactose with the highest percentage of fine particles: on average, 15.0% of the particles were smaller than 10 µm. Of the remaining lactoses, it is seen that all of them have a reduced percentage of fine particles, where LHα-sph had the lowest percentage of fine particles, around 0.86%. LHα-tom_sm has 2.95% and LHα-tom_lar 1.52% of particles smaller than 10 µm. The latter was expected considering LHα-tom_lar is the "larger version" of LHα-tom_sm, as shown in SEM images (section 3.1.2.), Figure 10(d) and the values of Span in Table 3.

As said before, a multimodal/heterodisperse carrier size distribution positively influences the performance of the drug. When a multimodal distribution is verified, it is expected that a higher percentage of fine particles are present in the powder[68]. A higher percentage of fine particles in carriers is imperative since it improves the DPI performance, and these are added into the formulation or could be present as "intrinsic fines". However, it is not known yet why and how the fine particles influence the DPI performance, existing several theories that try to explain this, as mentioned in section 1.4.2.2.1.[67]. According to Buttini *et. al*.[61], a minor quantity of fine lactose particles can be used in order to promote deaggregation of the drug powder. Likewise, fine lactose particles will adhere on to the larger carrier particles, reducing drug-carrier contact, facilitating drug dispersion and deposition, leading to a better aerosol performance.

Regarding the API, Figure 12(b), it is possible to see that around 89.00% of the SS particles are smaller than 10 µm, which confirms that most of the particles in the jet-milled sample were fine ones. Also, when the sample was analysed under a pressure of 0.1 bar, the percentage of fine particles was considerably lower, since SS particles were agglomerated, as already mentioned above. In general, the results obtained are consentient with the requirements found in literature for API PSD (Kaialy *et. al.*)[69].

The agglomeration of small particles is a regular phenomenon. Particles with higher percentage of fine particles tend to be more cohesive. For that reason, smaller particles such as API particles will have difficulties to disperse. To avoid the latter, two approaches can be employed: (1) controlled aggregation of the undiluted drug in order to obtain loosely adherent floccules; (2) mix fine drug particles with coarser carrier particles (approach used in this thesis)[70].

Adhesive blends are a formulation strategy for DPIs as carriers' particles can improve some of the characteristics of the micronized API. For example, the PSD and the particle surface characteristics of the carriers, can be used to influence and control the performance of the fine API particles, i.e. improve their flowability, increase dispersion during emission and improve dosing[40]. However, as already explained, only the API has the necessary aerodynamic diameter to reach the lungs[8,22].

According to Figure 12(c), SS+Lβ is the blend with the highest percentage of fine particles, followed by SS+LHα-tom_sm. The blend with the lowest percentage of fine particles is SS+LHα-tom_lar. When compared to the percentage of fine particles in the raw materials, an increased load of fines was seen, which is expected since the blends have 2% of SS. Examining carefully, on average, there is an increase of 4.22% of fine particles in SS+Lβ, 4.05% in SS+LHα-sph, 4.22% in SS+LHα-tom_sm and 3.75% in SS+LHα-tom_lar. Interestingly, this value is two times the expected 2% increase when the mentioned API load was mixed with the carrier. Thus, it is hypothesized that this might be due to the differences in powder bulk volume of the API in relation to the carrier particles; being that, it is expected that the micronized particles have a higher powder bulk volume than coarser ones[58,71], possibly explaining why more than a 2% increase was found.

Analysing the obtained results with the Span value in Tables 4 and comparing them with Figure 12(c), it is conclusive than higher values of Span are related to higher percentage of fine particles, since higher values of Span mean that the particle size has a heterodispersed distribution and it is notorious that blends have a considerable amount of particles smaller than 20 µm.

As certain amount of fines will undoubtedly help DPI performance, the blends trend as follows: SS+Lβ > SS+LHα-tom_sm > SS+LHα-tom_lar > SS+LHα-sph. Thus, in the next sections it will be analysed how the PSD can be correlated or not with powder hardness, flowability and *in vitro* aerodynamic performance.

Finally, to compare all the previous results, lactoses and SS were studied via wet dispersion, as well. Wet dispersion measurement complements dry dispersion analysis, by giving a clearer understanding when breakage/dispersion of agglomerates/particles occurs. That is, dispersion forces in wet dispersion are not so high and can offer an idea about the un-dispersed powder system[72]. In Figures 13 and 14 it is possible to see the $Dv_{0.5}$ results obtained by dry and wet dispersion to raw materials and blends, respectively.

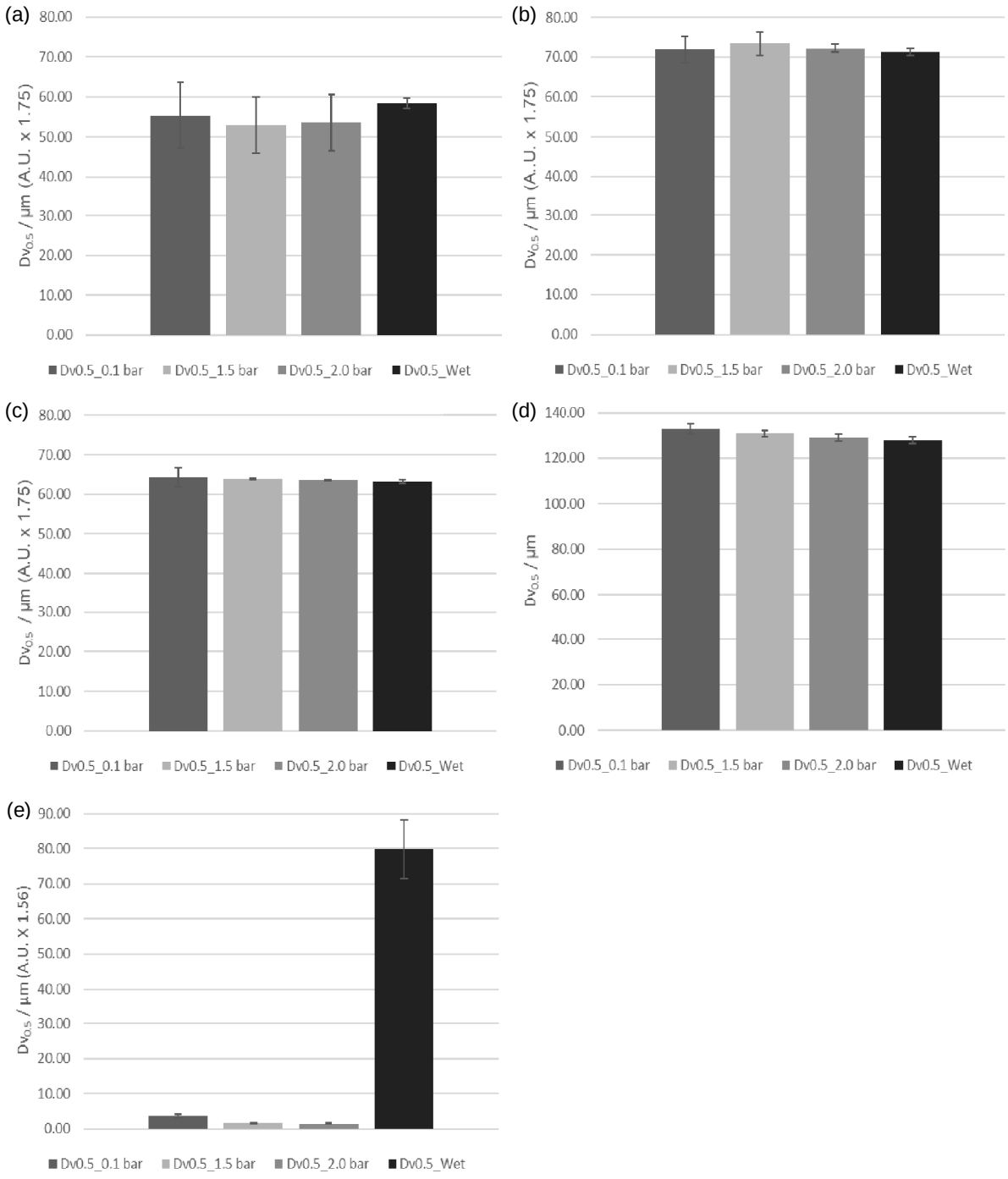

Figure 13 – Mean particle size values obtained via dry dispersion at primary titration of 0.1, 1.5 and 2.0 bar and mean particle size obtained via wet dispersion for (a) Lβ, (b) LHα-sph, (c) LHα-tom_sm, (d) LHα-tom_lar and (e) SS

Triplicates were carried out (Mean±SD)

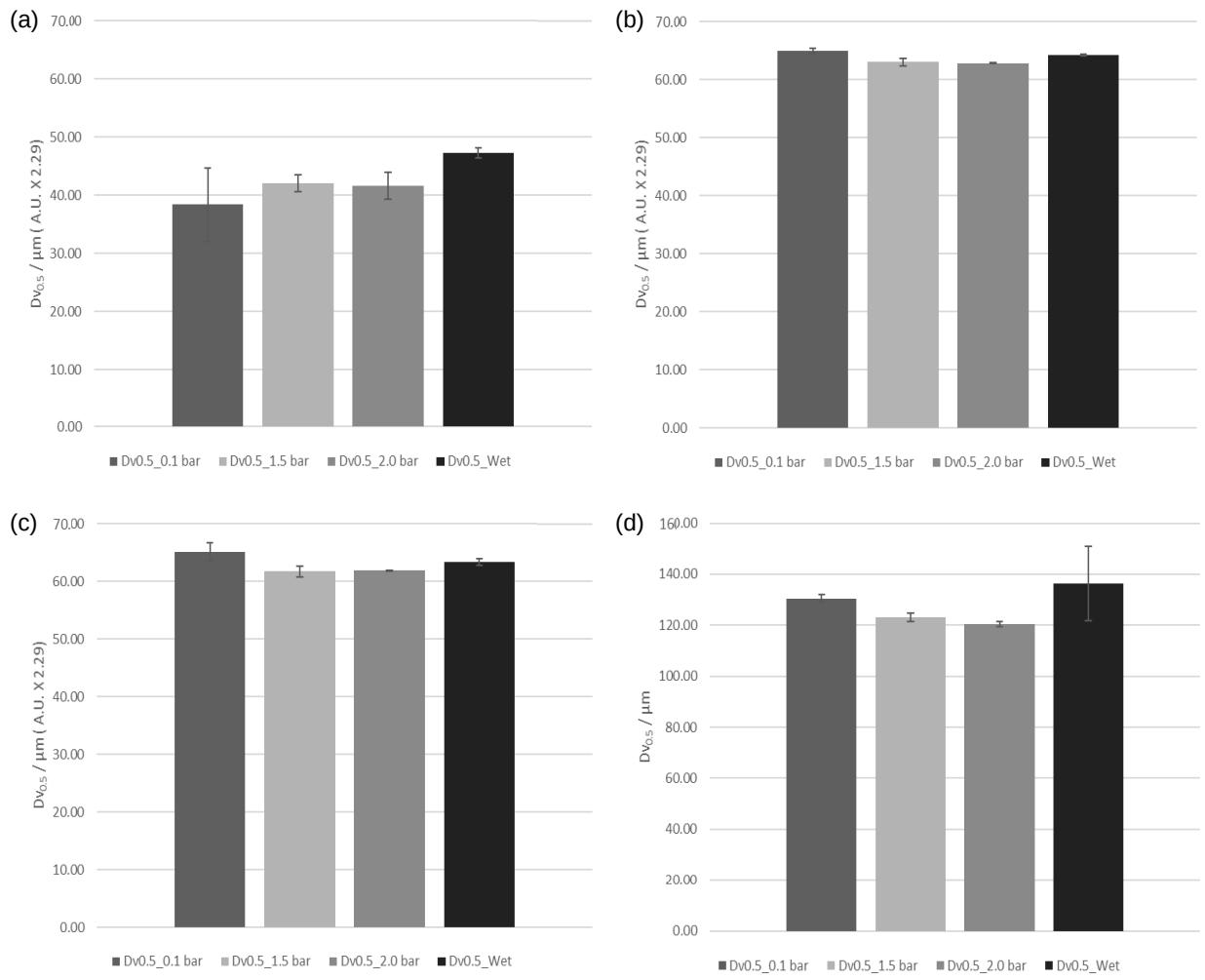

Figure 14 - Mean particle size values obtained via dry dispersion at primary titration of 0.1, 1.5 and 2.0 bar and mean particle size obtained via wet dispersion for (a) SS+Lβ, (b) SS+LHα-sph, (c) SS+LHα-tom_sm and (d) SS+LHα-tom_lar
Triplicates were carried out (Mean±SD)

Comparing the results of $Dv_{0.5}$ obtained by dry and wet dispersion, it is possible to withdraw some conclusions. Whenever the $Dv_{0.5}$ value obtained through wet dispersion were higher than dry dispersion ones, it indicated that the powders were composed of aggregates larger than single particles, being the case of Lβ, seen in Figure 13(a) ($Dv_{0.5}$_0.1bar = 55.41 ± 8.19 µm; $Dv_{0.5}$_1.5bar = 52.89 ± 7.09 µm; $Dv_{0.5}$_2.0bar = 53.57 ± 7.10 µm; $Dv_{0.5}$_wet = 58.45 ± 1.32 µm). This interpretation was supported by SEM images (section 3.1.2.) that indicated this was the case for Lβ. In the other three lactoses, $Dv_{0.5}$ values obtained by dry dispersion were lower or very similar to those obtained when the study was carried out in a wet dispersion mode, indicating that particle aggregates were not so prevalent. Moreover, API results supported the hypothesis that aggregates are not efficiently dispersed during wet-dispersion and that SS particles tendentially form large aggregates.

As already mentioned, SS particles (Figure 13(e)) tend to form large aggregates. These cohesive interactions, lead to agglomerated samples with a high surface energy and thus difficult to disperse[40,73,74]. As such, the addition of fine excipients can help buffer drug-drug interactions, avoiding the formation of strong API agglomerates that, otherwise, would have a detrimental effect on powder processability (i.e. mixing, capsule filling, aerodynamic performance)[74].

Regarding the blends (Figure 14), it is possible to see that the agglomerates are not breaking, which leads to bigger particles when the blends are studied. This can be explained by the fact that these blends have SS and, as already mentioned, micronized particles tend to be more cohesive and agglomerate with each other[74]. As seen before, the values obtained for SS by wet dispersion are extremely high, which can mean that the particles are not dispersing or not breaking. However, in this case, since the blends are homogeneous, these higher values found in wet-dispersion measurement can be explained by the fact that API particles are attached to the carriers' surface.

4.1.3. Hardness and Tensile Strength

The relation between the hardness and TS is proportional. The values of the hardness were obtained directly using a 3-in-1 hardness, diameter and thickness testing instrument (Table 5) and its representation can be found in Figure 15.

Table 5 – Hardness, thickness and diameter of the produced plugs using the raw materials and blends.

Material	Thickness (mm)	Hardness (N)
Lβ	3.54±0.24	8.54±1.36
LHα-sph	3.76±0.19	18.44±1.69
LHα-tom_sm	3.63±0.39	4.96±0.98
LHα-tom_lar	3.85±0.16	3.98±0.50
SS	2.29±0.15	46.84±7.81
SS+Lβ	3.48±0.07	21.98±6.25
SS+LHα-sph	3.57±0.11	63.40±7.59
SS+LHα-tom_sm	3.53±0.09	10.06±1.35
SS+LHα-tom_lar	3.39±0.26	4.58±1.30

Diameter (mm) = 10.00±0.00

5 replicates were carried out (Mean±SD)

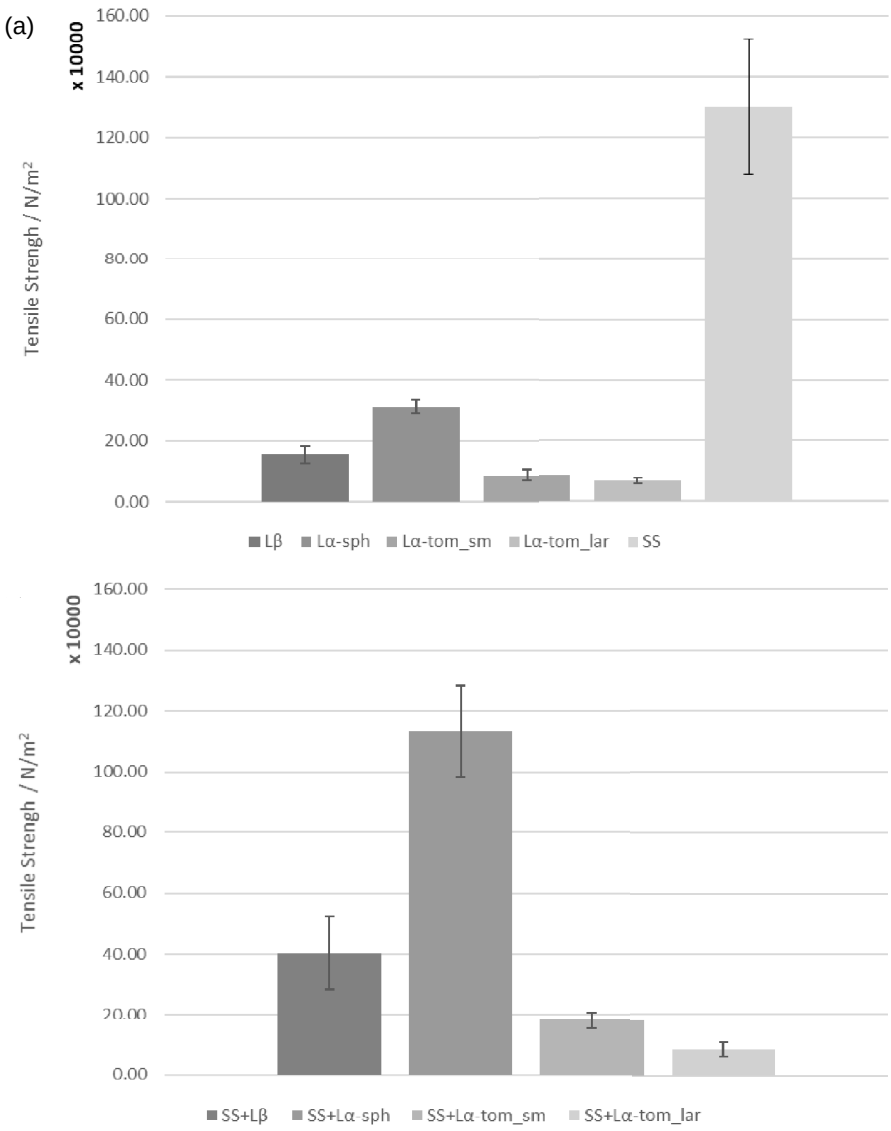

Figure 15 – Tensile strength (N/m^2) of (a) carriers, API and (b) Blends
5 replicates were carried out (Mean±SD)

Conforming to Figure 15(a), LHα-sph is the lactose with the highest value of TS (TS=312230.24±21125.13 N/m^2), while LHα-tom_sm (TS=87382.51±18925.24 N/m^2) and LHα-tom_lar (TS=65956.00±9112.71 N/m^2) have the lowest values. Ranking all the raw materials results that SS > LHα-sph > Lβ > LHα-tom_sm > LHα-tom_lar.

In terms of particle shape, it is possible to say that spherical particles have a minor tendency to deform/break, because they compact in a more cohesive way[38], which leads to a higher value of TS for LHα-sph. Non-regular particles, which is the case of Lβ, LHα-tom_sm and LHα-tom_lar, tend to deform/break more easily. Besides particle shape, also particle size and the percentage of fines have a central importance in the obtained results. When analysing the SS result, it is evident that is the raw material with the highest value of TS and this result from the fact that SS has a greater percentage of fine particles. Also, although these particles have the

same particle shape, there is a small difference between the TS obtained for LHα-tom_sm and LHα-tom_lar, in which the first one has the higher value. This result is due to the percentage of fines present in each of the lactose particles: LHα-tom_sm has the highest percentage of fine particles when compared with LHα-tom_lar (2.95%, on average, according to Figure 12(a)) and, naturally, has a higher TS associated.

According to the fluidization theory, a bigger percentage of fines lead to a higher TS, which is directly related to the interparticulate forces and the free volume of the carrier: the greater the interparticulate forces, the higher the TS[71]. It is also known that powder flowability, packing properties and tensile strength have a drastic effect on powder fluidization and, consequently, in aerodynamic performance, increasing the aerodynamic drag force applied to fluidize the powder bed.

In the case of the blends, represented in Figure 15(b), it is possible to rank them: SS+LHα-sph > SS+Lβ > SS+LHα-tom_sm > SS+LHα-tom_lar, which is the expected ranking, considering the results for the raw materials used in these blends. Likewise, the values of TS are now higher, which is expected as well. It is proposed that this occurs due to the exposure of smaller drug particles at the carrier surface, leading to the creation of solid bridges, resulting in a more compact agglomerate, which results in higher values of hardness/TS[75]. Moreover, when there is a higher percentage of fine particles, it is expected that more contact points exist and when the powder was compressed, a plastic deformation led to an increase of the contact surface area between API and carrier particles, increasing the adhesion force[76].

4.1.4. Density and Porosity

Since the TS was measured, understanding what was happening with porosity was an essential parameter to analyse. The results are represented in Figure 16.

Ranking the raw materials in terms of porosity, results that LHα-tom_sm > Lβ > LHα-tom_lar > LHα-sph > SS. Therefore, it seems to exist a relation between the hardness/TS and the porosity: higher values of hardness correspond to lower value of porosity, in general. As described in the literature, TS is a function of the cohesive forces at the contact points and an inverse function of both particle diameter and its porosity[38]. It is visible, in Figure 16(a), that LHα-sph presented the lowest value of porosity among the lactoses and this happened due to the fact that it has a spherical shape. This lead to a more organized disposition of the particles, presenting uniform packing arrangement with higher powder bed TS, which reduces the porosity of the powder[63].

Badawy *et.al.*[77] have demonstrated that particle size of the carriers is related with the porosity as well: when the carrier particles are smaller, its porosity tends to be higher since they showed a reduced tendency for densification. Increasing the particle size, a less porous powder is obtained because there is a decrease in both capillarity and viscous interparticle

forces which leads to a more deformable particle. According to Figure 16(a), it is possible to see a relation between the smaller particle size and the higher value of porosity. However, concerning the API, this principle cannot be applied, since SS is the raw material with the smallest particles, being micronized and compacting better.

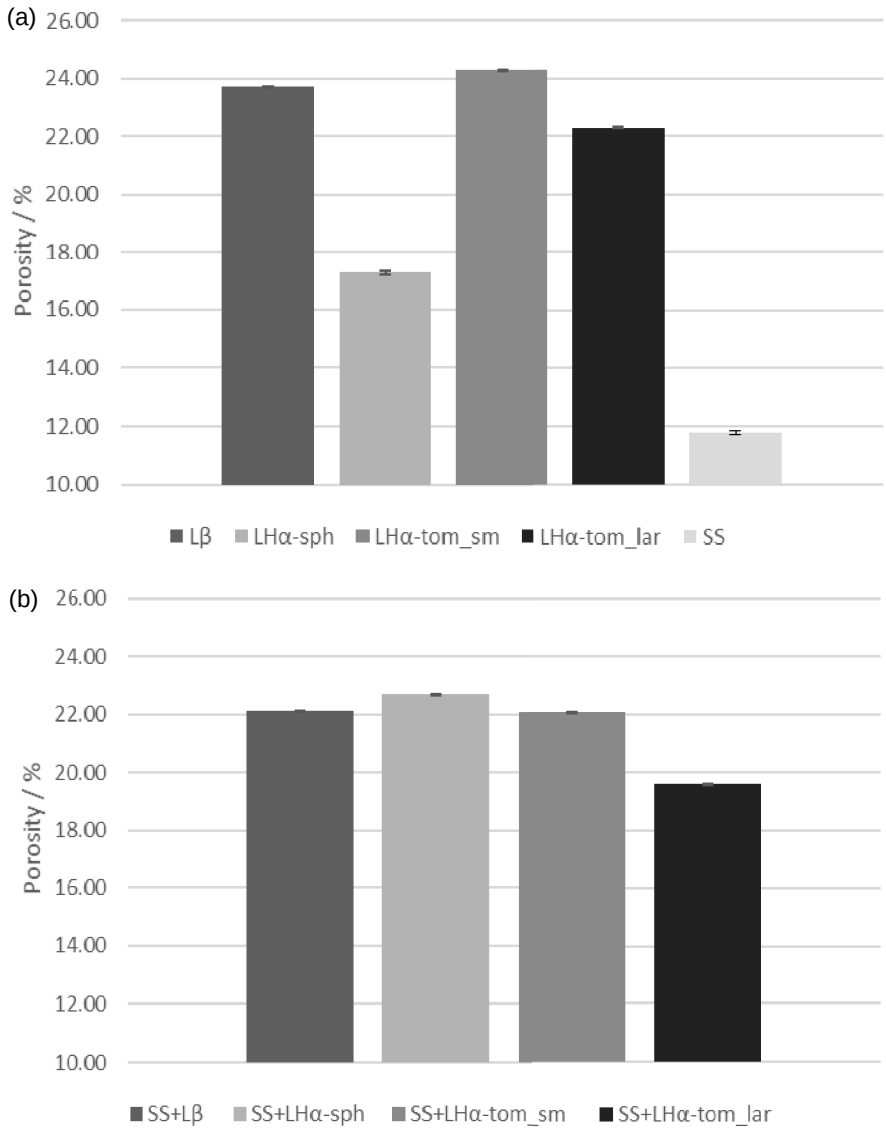

Figure 16 – Porosity, in percentage, of the (a) carriers, API and (b) produced blends
5 replicates were carried out (Mean±SD)

Concerning the blends represented in Figure 16(b), the porosity values are not inversely proportional to those obtained for the hardness, at least regarding the SS+LHα-sph, contrary to what was initially expected. In this case, SS+LHα-sph has the highest value of porosity, although being expected to have the lowest value of all the blends, and the remaining blends have now a slightly lower value of porosity. Considering the literature, after the exposure of the lactose to fine particles, solid bridges between both materials are formed, resulting in a more

compact and less porous agglomerate[75], as already explained before. This was the case in SS+Lβ, SS+LHα-tom_sm and SS+LHα-tom_lar.

According to Zeng *et. al.*[38], compressing a powder can create several artefacts since compression may alter some of the intrinsic properties of the materials and this could be the reason why SS+LHα-sph results are different from what was expected. Moreover, SS can also alter the properties of the lactoses, namely their porosity. To be sure about what is changing, further studies are required. For example, SEM images of the compacted blends can elucidate about the presence of any particle changes after compression. Compression might have changed the shape of the carrier, causing a change in its porosity, i.e. when compressed at a specific pressure, the particles may have changed their shape in the presence of SS, to a smaller value of bulk density, smaller tap density and higher porosity[78].

4.1.5. Compressibility, Permeability and Cohesivity

Compressibility

The powder bulk properties were also analysed in order to understand how powder properties influence these results. First, a compressibility test was conducted, and the results are represented in Figure 17.

Lβ is the lactose with the highest value of compressibility and SS has the highest value of compressibility of all the powders studied. The percentage change in volume after compression (CPS) tends to increase with the increase of the applied pressure. The behaviour of powders under compression can be used as a generic criterion for powder flowability. Cohesive powders have an aleatory packing and compress easily, which means they have poor flowability[71]. As already mentioned, a higher percentage of fine particles in a powder turns the powder more cohesive[70] and, actually, it is possible to see that the raw materials with higher percentage of fines, which correspond to the ones with higher value of Span, are those that have a higher value of compressibility. It is also reported in the literature that the presence of fine particles increases the cohesive interparticulate forces inside the powder bed and affects the TS, increasing it as well. When an increasing consolidation stress is applied to the powder, the TS of a cohesive material will increase, impacting on fluidization and overall performance of DPI formulation[71].

The surface geometry and the physical behaviour of the granules influence the compressibility results. Surface roughness, for instance, can largely explain these results; that is, a rougher surface leads to a greater value of compressibility[38]. Analysing the values of the surface area of all the carriers in section 3.1.2, Table 1, Lβ is the carrier with the highest value of SSA, which supports the former.

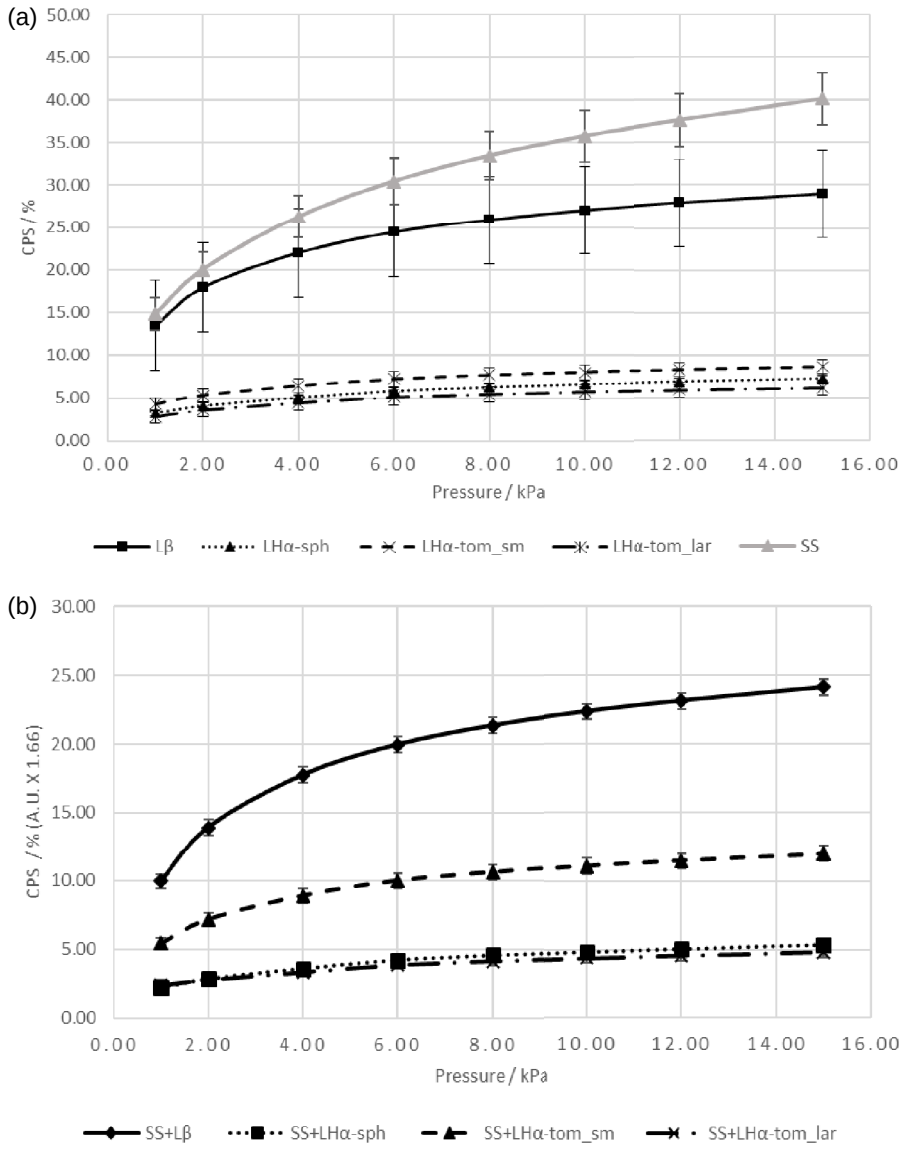

Figure 17 – Percentage change in volume after compression for (a) carriers, API and (b) blends at different pressures applied from 1 to 15 kPa
Triplicates were carried out (Mean±SD)

Since one of the ways to decrease the cohesion and, consequently, the agglomeration of fine cohesive particles, is to blend coarse lactose carriers with API, the compressibility was also tested for the blends. According to Figure 17(b), it is evident that SS+Lβ has the highest value of compressibility and that SS+LHα-sph and SS+LHα-tom_lar are the blends with the lowest values. Although the ranking of compressibility is the same as that for the raw materials, it was evident that the addition of SS to LHα-tom_sm had a greater effect than in the other lactoses. As known, LHα-tom_sm has a small SSA, relatively high percentage of fines and a wide PSD, as it is possible to confirm in the previous tests. For these reasons, LHα-tom_sm

has less space available to SS to adhere to its surface, which means these particles of API will be closer to each other, increasing the cohesivity of the blend[38,71].

According to Santl *et. al.*[79], wider PSD contribute to a denser packing of the particles, leading to higher values of compressibility. As seen before, higher values of Span mean wider PSD and SS+Lβ has the wider PSD of all the blends and, as expected, have the higher values of compressibility as well. Thus, considering this theory, it was expected that SS+LHα-sph would have the second higher value of compressibility. However, this was not verified since in materials with high tendency to fragment (such as the spherical particles), the original particle size is less important than for plastic or non-fragmenting materials[79].

Permeability

The permeability of the powders was tested as well, in order to understand the effect of the bulk powder properties on the fluidization properties. This measure demonstrates how easily the material can transmit a fluid, air in this specific case, through its bulk. The process is very similar to the compressibility, but in this case a quantity of air goes through the sample during the compression (Figure 18). The results represented below are in values of Pressure Drop (PD) and not in permeability itself. So, it is important to consider that PD and permeability have an inverse relation; in other words, when the value of PD increases, the value of permeability decreases.

According to Figure 18(a), it is possible to assume that Lβ has the lowest values of permeability (higher values of PD), which means that it is the lactose with less "free spaces" between particles. Therefore it is enlightening that the smaller the particle size, the smaller the permeability of the powder, resulting in an inverse proportionality between compressibility and permeability[71]. LHα-tom_lar, being the lactose with the biggest particles, has the highest values of permeability (lowest values of PD). According to Cordts and Steckel[80], the values for the PD across the powder bed can be correlated to the overall fine content, so the more fines found in the sample, the smaller the permeability value at a given applied normal stress. With the increase of the compression, the empty spaces between the particles will become smaller and smaller, leading to an increase in resistance to air throughput. Hence, the behaviour seen for SS can be explained by this and, as a result, the air is not free to permeate through the powder bed and the airflow permeate through channels formed within the powder bed[71].

Moreover, according to Shalash *et. al.*[81], in addition to the percentage of fines, the permeability of the powder bed is also associated to PDS, shape, porosity, cohesivity, compressibility and TS. As represented in Table 3, SS is the raw material with higher value of Span, followed by Lβ. Having higher values of Span, they have a wider PSD which leads to a lower permeability and a higher compressibility and cohesivity, since they have also a higher percentage of fine particles, turning the material more cohesive.

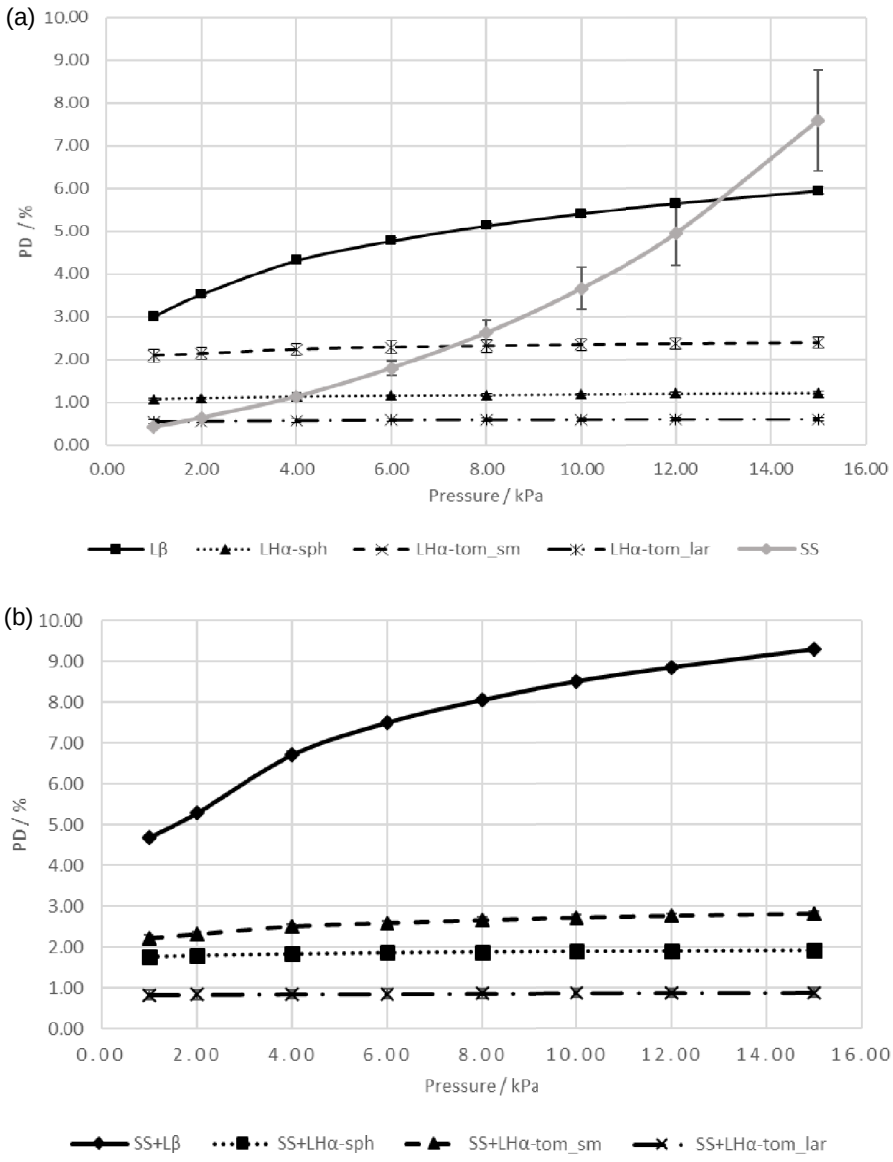

Figure 18 – Pressure drop variation for (a) carriers, API and (b) blends at different pressures applied from 1 to 15 kPa, with a constant airflow velocity of 2 mm.s^{-1}
Triplicates were carried out (Mean±SD)

Naturally, as seen in Figure 18(b), SS+Lβ is the blend with the lowest value of permeability. SS+LHα-tom_lar, where a blend with the largest particles was produced, the highest values of permeability were found. So, it is possible to say as well that the ranking of permeability remains the same in Figure 18(b). Cordts and Steckel[80] supported these results, where the authors related the percentage of existing fine particles with the PD value, which means that the higher the amount of fines, the lower the permeability.

Studies about the relationship between the permeability and the DPI performance have shown that performance improves when the permeability of the carrier or the inhalation mixture decreases. However, for turbulent-shear inhalers, there are some authors that find this

relationship very complex[81]. According to one of the theories to explain the relation between the amount of fine particles and the aerodynamic performance of DPI is said that fluidization of a DPI occurs when the PD across the powder bed is equivalent to the weight of the powder. So, the addition of fines improves DPI performance by increasing the TS of the formulations, which is related to the interparticulate forces and the free volume of the carrier. This means than when the permeability of the blend is lower, there is a higher amount of fines associated to that blend and it presents a better aerodynamic performance, which is expected to be the case for SS+Lβ.

Cohesivity

In order to investigate the tendency that each material/blend has for interparticle interactions, a shear cell test was conducted, and the results are represented in Figure 19.

The lactose with the highest value of cohesivity is Lβ, according to what is represented in Figure 19(a). Thus, it can be said that there is a direct proportionality relation between compressibility and cohesivity, which also indicates a correlation with the particle size of the powders studied. Hence, it is possible to say that smaller particles tend to have higher values of cohesivity, having a higher interparticulate force, which explains why SS has the highest values of cohesivity, followed by Lβ. However, in this case, it is possible to see that LHα-sph is the less cohesive material. So, the ranking of cohesivity is SS > Lβ > LHα-tom_lar > LHα-tom_sm > LHα-sph. According to Kou *et.al*.[82], roughness and morphology are a key aspect to understand the cohesion of the materials. If the material is rough, the cohesion is higher and if the particles are spherical, the cohesion is lower, which explains why LHα-sph is the least cohesive material, since it is rough but spherical. Also, it is known that spherical particles have a higher flowability when compared with irregular particles, due to less interparticle contact points[31,58], which reduces the aerodynamic performance of DPIs[31]. Also, it is visible that the values of cohesivity are very similar between LHα-tom_sm and LHα-tom_lar, since they just differ in their size and, for this specific parameter, size is not as relevant as roughness and morphology.

Considering Figure 19(b), the ranking of cohesivity is the same as Figure 19(a), which means that SS+Lβ is the blend with the highest values of cohesivity and SS+LHα-sph has the lowest values of all the four blends. Although, blends have higher cohesivity values. According to Leuenberg *et. al.*[83], the cohesion between fine drug particles and coarse carrier particles increase and the interactive forces, such as the Van der Waals attractive force between the mixed powder particles increase. This increase influences the aerodynamic performance of DPIs, improving the performance, since Van der Waals forces are very weak and allow the API to detach more easily from the coarse carrier. Furthermore, it is visible that smaller and more irregular particles have higher values of cohesivity and the spherical ones are those with

less cohesivity, which is concordant with the results found in literature[82]. Irregular and smaller particles tend to have more contact points, which allows a greater “connection” between the particles during the mixing.

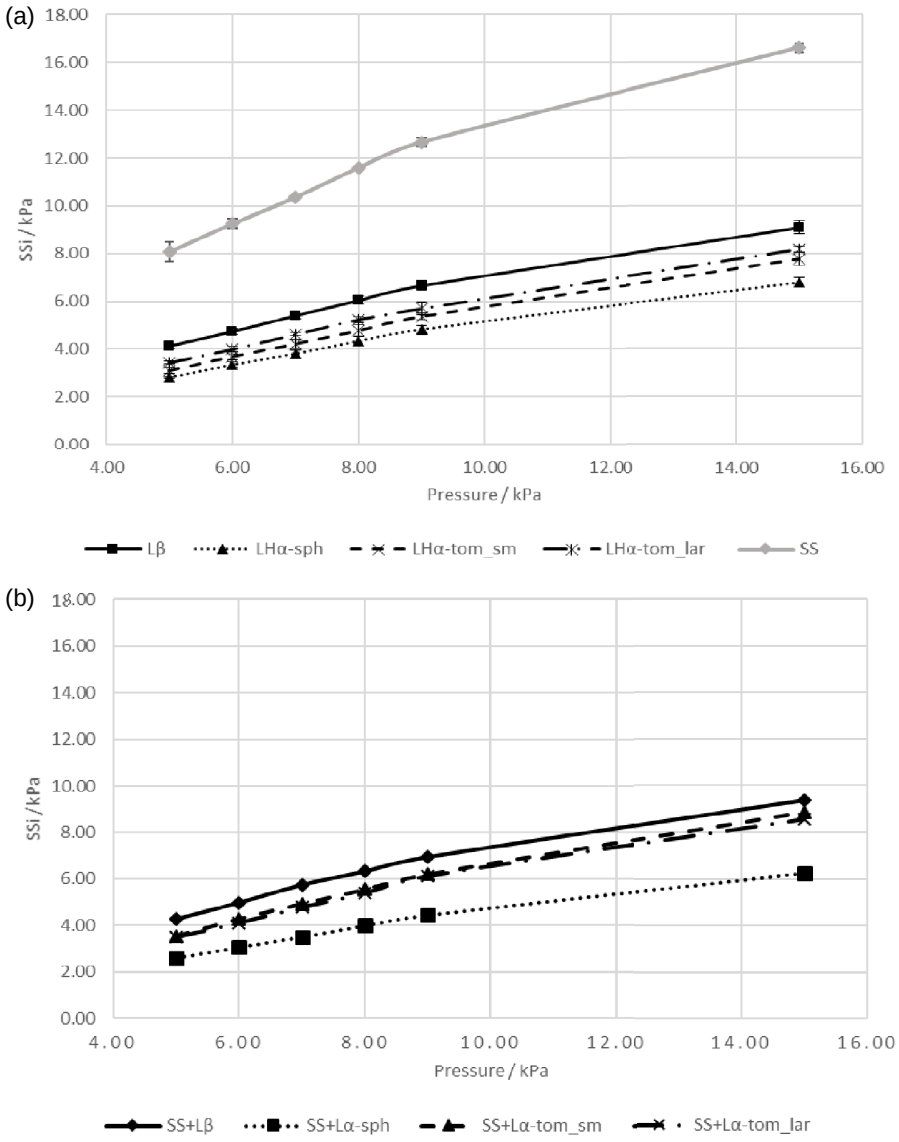

Figure 19 – Supersonic shear imaging for (a) carriers, API and (b) blends at different pressures applied from 5 to 15 kPa
Triplicates were carried out (Mean±SD)

It was confirmed that a higher percentage of fines can increase compressibility, decreasing the air permeability of the powder bed. The effect of fines leads to a better aerodynamic performance of DPIs[71], which means that materials that compress better have better results in aerodynamic performance, as well.

4.1.6. Aerosolization Performance

After the evaluation of the particle characteristics and bulk properties, *in vitro* aerosolization performance was performed. As already mentioned in section 1.4.3.2., this *in vitro* test allows the determination of the *in vivo* action of the formulation, simulating the aerosol deposition into the lungs[61].

It is known that several properties influence the aerodynamic performance of DPIs, such as the percentage of fine particles, permeability and compressibility of the materials used in the formulation, shape of the particles, etc.[40,80,84]. Which was important to know now was to understand which property most influence these results. For that, API particles were separated according to their cut-off diameters, as represented in Table 6.

Table 6 – Cut-off diameters of the individual stages at 60 and 100 L/min

Stages	60 L/min	100 L/min
S1	6.12	8.06
S2	3.42	4.46
S3	2.18	2.82
S4	1.31	1.66
S5	0.72	0.94
S6	0.40	0.55
S7	0.24	0.34
S8	<0.24	<0.34

Table 7, represented below, include the parameters describing the aerodynamic performance of the four blends at both flow-rates. The emitted dose (ED) represents the quantity of powder that came out of the device and capsules, its correspondent value in relation to the total dose of API – the emitted dose of the dose (EDD), the FPF and its correspondent value in mass (FPD), as well as the MMDA were calculated in accordance to the US Pharmacopeia.

For all the blends studied, the results concerning the EDD were very similar, being these between 82-105%, meaning that no notable differences were found regarding this parameter between both flow-rates. Also, all the blends, except SS+LHα-sph, presented an EDD below the total amount of SS in the blends, which implied that a certain quantity of SS remained in the capsules and/or in the inhalation device. It is known that large intra- and inter-inhaler dose emission differences may result in asthma and COPD exacerbations and this may also occur due to the absence of immediate therapeutic feedback during inhalation[84]. So, it is very

important that the EDD value are still the same regardless the flow-rate used, since not all the patients are able to achieve the same flow-rate values during inhalation.

Table 7 – Aerodynamic performance results (ED, EDD, FPD, FPF and MMAD values) of the four blends at 60 and 100 L/min

Blends	ED (µg)	EDD (%)	FPD (µg)	FPF (%)	MMDA (µm)
60 L/min					
SS+Lβ	2746.03 ± 0.08	84.61 ± 2.48	956.29 ± 0.01	34.83 ± 0.77	3.20 ± 0.20
SS+LHα-sph	3387.84 ± 0.03	105.15 ± 0.83	178.22 ± 0.02	5.26 ± 0.58	2.88 ± 0.08
SS+ LHα-tom_sm	2815.95 ± 0.14	87.37 ± 3.75	757.92 ± 0.03	27.00 ± 2.48	2.51 ± 0.13
SS+ LHα-tom_lar	2636.72 ± 0.16	82.05 ± 4.62	413.06 ± 0.03	15.71 ± 1.52	2.33 ± 0.05
100 L/min					
SS+Lβ	2687.6 ± 0.03	83.59 ± 0.76	963.34 ± 0.04	35.84 ± 1.27	2.60 ± 0.10
SS+LHα-sph	3412.13 ± 0.07	105.79 ± 1.94	255.78 ± 0.05	7.51 ± 1.60	3.10 ± 0.85
SS+LHα-tom_sm	2867.68 ± 0.05	89.06 ± 1.57	924.67 ± 0.03	32.25 ± 1.44	2.37 ± 0.11
SS+LHα-tom_lar	2743.19 ± 0.09	85.18 ± 2.78	641.64 ± 0.03	23.41 ± 1.46	2.08 ± 0.06

Triplicates were carried out (Mean±SD)

Besides the EDD, the main parameter that affects the DPI efficacy is the FPF. In general, it is possible to see that a flow-rate of 100 L/min led to higher values of FPF. However, for SS+Lβ and SS+LHα-tom_sm almost no difference could be found between the used flow-rates. Since not every patient is able to achieve the same flow-rate during inhalation and, as said before, the same amount of API should reach the lungs regardless the inhalation capacity of each person, the aforementioned observation indicated that Lβ and LHα-tom_sm could be advantageous for DPI performance. It was also evident that blends with higher values of fine particles had the best results concerning FPF, which according to the literature was to be expected. According to Grasmeijer *et. al*.[85] and Guenette *et. al.*[67], a constant positive relationship exists between fine lactose content of different blends and the FPF of SS for cut-off values lower than 10 µm. It is well-known that fine particles improve the performance of DPIs, however the reason why this is so is still under discussion (section 1.4.2.2.1.). For example, one of the theories says that the carrier has areas which are more adhesive than others and they are occupied by fines, leaving the less energetic spots to API fines, which leads to an easier detachment from the carrier surface[40]. In turn, SS+LHα-sph blends had the lowest FPF. It is speculated that SS+LHα-sph blends form powder beds that break as plugs or

fractures instead of an aerosol cloud, as such the API cannot reach the lungs. It is known that spherical particles tend to be more cohesive, having a uniform packing arrangement with higher TS (as demonstrated in section 4.1.3.). These type of particles is difficult to fluidize via airflow, resulting in an inferior and variable lung deposition of fine particles[63]. Moreover, the big pores and roughness at the surface of the carrier might have provided shelter for the API particles to be shield against fluidization forces[63]. Thus, it was no surprise that this carrier showed a markedly worst aerodynamic performance.

According to Table 7, comparing the performance of the SS+LHα-tom_sm and SS+LHα-tom_lar it was also possible to conclude that particles of the same shape and similar roughness led to worse results of aerodynamic performance. A possible explanation for the former is that larger carrier particles exhibit higher press-on forces during mixing with micronized API, due to their larger mass and inertia, resulting in stronger adhesive forces[86]. In addition, lactose powders with irregular shape and rough surface are expected to have lower Van der Waals interparticulate forces, dispersing better upon aerosolization[87]. Furthermore, blends of API with these type of lactose powders are expected to have a higher porosity, lower permeability and higher cohesivity, as well as compressibility. Therefore, these confirmed the hypothesis proposed in section 4.1.5. and a better aerodynamic performance were seen in the case of this type of blends (SS+Lβ and SS+LHα-tom_sm).

Another important parameter to consider after aerodynamic analysis is the MMAD. Larger values of MMAD are expected for aerosolizing blends where drug agglomerates are present[63]. Thus, naturally, MMAD values differ regarding the flow-rate used. In line with the fracture hypothesis proposed above, at 100 L/min, SS+LHα-sph was the blend with larger MMAD, resulting in the smallest value of FPF among the tested blends. However, at 60 L/min, SS+Lβ had the highest value of MMAD, which was not expected. Hence, further research is needed in order to understand more in-depth how the flow-rate affected the MMAD. LHα-sph has a regular shape (spherical) and a rough surface, since has deep gaps and large pores and this structure contributed to the aerosolization performance[63].

In Figure 20 it is possible to confirm what was said when analysing the previous tables. These plots illustrate the deposition of SS particles in the different stages of the impactor for a flow-rate of 60 L/min and 100 L/min.

It was evident that most of the SS particles impacted in the pre-separator. This might be explained by the fact that a high percentage of those particles were attached more tightly to the carrier surface and as such, not able to detach during inhalation. Consequently, these high SS content in the pre-separator led to not even 50% of the drug being able to reach the lower stages of the NGI.

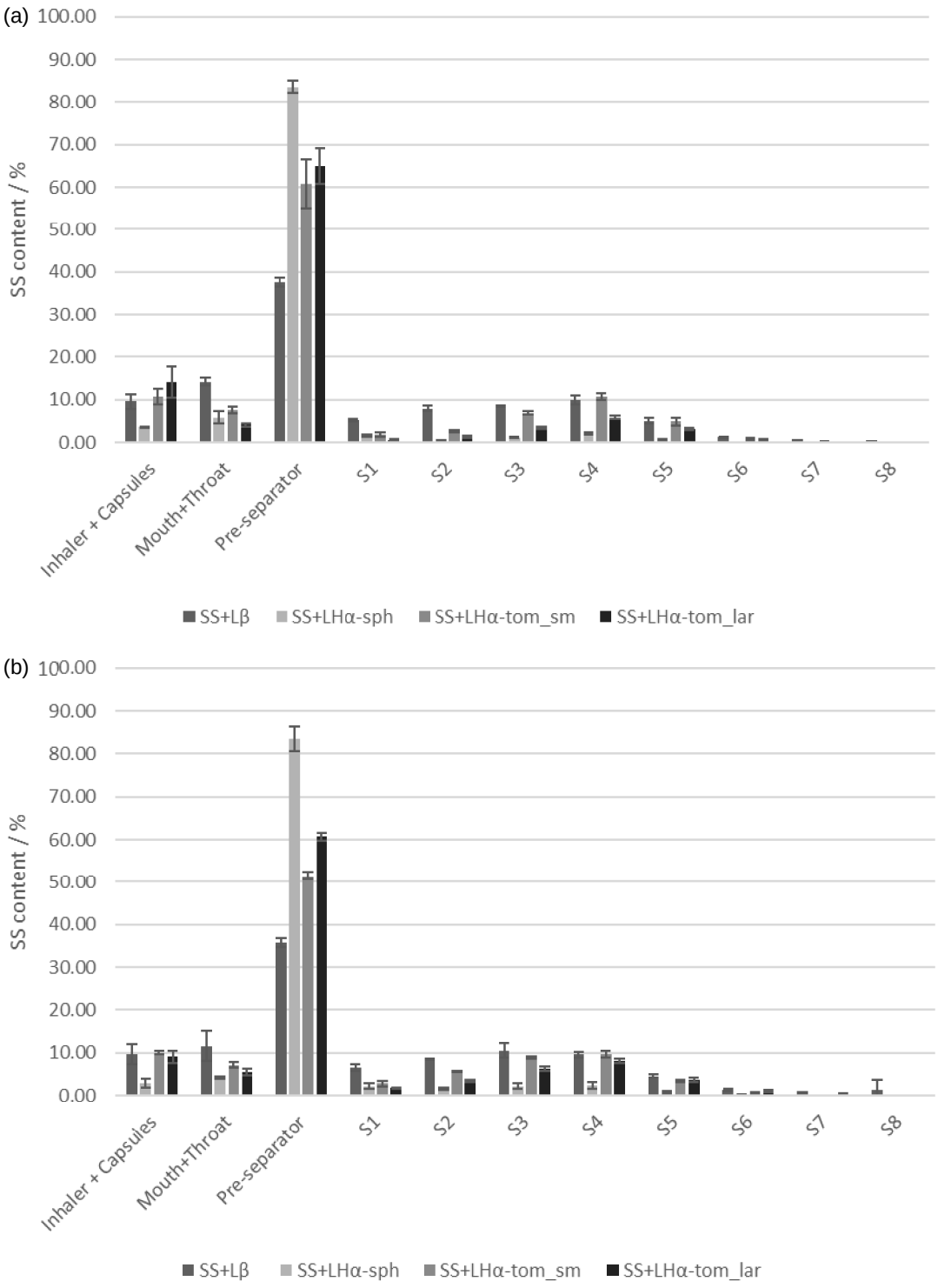

Figure 20 - Amount of SS (w%) deposited on the inhaler device + capsules shells, mouthpiece+throat, pre-separator and different stages after aerosolization of the DPI blends, operating at a flow-rate of (a) 60 L/min and (b) 100L/min

Triplicates were carried out (Mean±SD)

For both flow-rates it was visible a superior and constant *in vitro* aerosolization performance for the Lβ blends. This can be partially explained due to its elongated shape, greater SSA, greater percentage of fine particles, lower permeability and higher compressibility and cohesivity values, leading to a better detachment of API particles from the carrier[88].

Therefore, considering all the results obtained, it is possible to say that the percentage of fine particles is the property which contributes the most to a better aerodynamic performance of DPIs. However, the former is not the only property that should be considered when deciding which carrier to be used in a DPI formulation, in order to obtain a good performance. As an example, a bigger percentage of fines lead to a higher TS, which is related to the interparticulate forces and the free volume of the carrier: the greater the interparticulate forces, the higher the TS[71]. Also, powder flowability and packing properties are influenced by the percentage of fines, having a drastic effect on powder fluidization and, consequently, in aerodynamic performance, which can be confirmed by analysing Table 7 and Figures 20 (a) and (b).

5. CONCLUSION

The present work confirmed that different particle characteristics, such as particle size, shape and morphology, produced powder beds with distinct adhesive and cohesive properties, affecting the flowability, compressibility and permeability of the produced blends. Moreover, *in vitro* testing using an NGI elucidated how particle and powder bulk properties can influence the aerodynamic performance. It was hereby confirmed the importance of particle size, shape and percentage of fines, showing how carrier particles can be engineered to improve DPI performance.

After confirming that all the produced blends exhibited the intended mixing homogeneities, they were used for further *in vitro* testing. Powder bulk characterization displayed that different blends have different behaviours in terms of compressibility, permeability and cohesivity, showing that the characteristics of the powders influence these powder bulk properties. For instance, the best blend studied, presenting the best aerodynamic performance, was SS+Lβ. This presented higher compressibility and cohesivity, as well as lower permeability. The former was shown to be dependent of the particle size of the carrier, as well as its shape.

Also, the TS and porosity were studied showing the expected results: spherical particles, which is the case of the LHα-sph, had a higher value of TS, when comparing with more non-regular particles. Between TS and porosity an inverse relationship was found, which means that LHα-sph was the least porous lactose studied. However, this relation was not verified when the blend was analysed and, for that reason, further investigations are required.

Two different flow-rates were tested, 60L/min and 100L/min, to understand how the aerosol deposit in the lugs. The best results were obtained for SS+Lβ. The superior aerodynamic performance of this blend could be justified by its higher percentage of fine particles, as well as the non-regular shape of Lβ, possibly leading to easier API detachment during aerosolization. Additionally, FPF, ED values, as well as SS content in the different stages were constant regardless of the flow-rate used. This reveals the advantage of using carriers with similar properties to Lβ, since the delivered dose of API should be the same regardless the flow-rate generated by the patient. The worst aerodynamic performance was obtained for SS+LHα-sph. The spherical morphology of this carrier and correspondent higher TS, as well as its big pores and gaps at the surface made fluidization difficult and enabled the small API particles to be sheltered against aerosolization forces, respectively.

Taking into account all the findings and confirmations in the present work, it can be stated that a higher percentage of fine particles is a critical parameter to consider for capsule based DPI devices, since it influences all of the properties studied and leads to a better aerodynamic performance. Thus, it is also proposed that a carrier with similar properties to the ones found

for the Lβ can be advantageous in the production of capsule based DPI formulations. Therefore, it is possible to confirm the hypothesis initially established in this thesis.

6. FUTURE PERSPECTIVES

Some aspects of this work need further investigations to understand clearly some important results.

As said, the result concerning the porosity of SS+LHα-sph was not expected. In order to understand this inconsistency, morphology and surface tests should be conducted. Alternatively, plugs should be produced using different pressures to understand if there is a point beyond which the characteristics of the powder actually change.

As the worst result of aerodynamic performance was obtained for SS+LHα-sph, it was presumed that the spherical morphology of this carrier and correspondent higher TS, as well as its big pores and gaps at the surface, made fluidization difficult and enabled the small API particles to be sheltered against aerosolization forces. However, further research is needed to prove these statements, i.e. SEM images after NGI performance.

Also, in order to obtain more precise results concerning the TS and porosity, the bulk density of the materials should be measured instead of calculated.

Moreover, to be sure about the contributions of all particle and bulk properties in DPI performance, a multivariate analysis should be conducted.

BIBLIOGRAPHY

1. Aulton ME, Taylor KMG. *Aulton's Pharmaceutics - The Design and Manufacture of Medicines, 4th Ed*.; 2013.
2. Labiris NR, Dolovich MB. Pulmonary drug delivery. Part I: Physiological factors affecting therapeutic effectiveness of aerosolized medications. *Br J Clin Pharmacol*. 2003;56(6):588-599. doi:10.1046/j.1365-2125.2003.01892.x.
3. Zeng XM, Martin GP, Marriott C. The controlled delivery of drugs to the lung. *Int J Pharm*. 1995;124(2):149-164. doi:10.1016/0378-5173(95)00104-Q.
4. Pilcer G, Amighi K. Formulation strategy and use of excipients in pulmonary drug delivery. *Int J Pharm*. 2010;392(1-2):1-19. doi:10.1016/j.ijpharm.2010.03.017.
5. Traini D. Inhalation Drug Delivery. In: *Inhalation Drug Delivery: Techniques and Products*. ; 2013:1-14. doi:10.1002/9781118397145.ch1.
6. Johnson RL, Hsia CCW. Anatomy and physiology of the human respiratory system. *Hum Respir*. 2006;24:1-29. doi:10.2495/978-1-85312-944-5/01.
7. Williams RO, Carvalho TC, Peters JI. Influence of particle size on regional lung deposition - What evidence is there? *Int J Pharm*. 2011;406(1-2):1-10. doi:10.1016/j.ijpharm.2010.12.040.
8. Dickhoff BHJ, De Boer AH, Lambregts D, Frijlink HW. The effect of carrier surface and bulk properties on drug particle detachment from crystalline lactose carrier particles during inhalation, as function of carrier payload and mixing time. *Eur J Pharm Biopharm*. 2003;56(2):291-302. doi:10.1016/S0939-6411(03)00109-7.
9. Islam N, Gladki E. Dry powder inhalers (DPIs)-A review of device reliability and innovation. *Int J Pharm*. 2008;360(1-2):1-11. doi:10.1016/j.ijpharm.2008.04.044.
10. Alagusundaram M, Deepthi N, Ramkanth S, et al. Dry Powder Inhalers - An Overview. *Int J Res Pharm Sci*. 2010;1(1):34-42.
11. Stuart BO. Deposition and Clearance of Inhaled Particles. *Environ Health Perspect*. 1984;55:369-390. doi:http://dx.doi.org/10.1016/B978-012352335-8/50089-2.
12. Yeh HC, Phalen RF, Raabe OG. Factors influencing the deposition of inhaled particles. *Environ Health Perspect*. 1976;Vol.15(June):147-156. doi:10.1289/ehp.7615147.
13. Hou S, Wu J, Li X, Shu H. Practical, regulatory and clinical considerations for development of inhalation drug products. *Asian J Pharm Sci*. 2015;10(6):490-500. doi:10.1016/j.ajps.2015.08.008.
14. Ashurst I, Malton A, Prime D, Sumby B. Latest advances in the development of dry powder inhalers. *Pharm Sci Technolo Today*. 2000;3(7):246-256. doi:10.1016/S1461-5347(00)00275-3.
15. Newman SP. Dry powder inhalers for optimal drug delivery. *Expert Opin Biol Ther*.

2004;4(1):23-33. doi:10.1517/14712598.4.1.23.

16. Rogliani P, Calzetta L, Coppola A, et al. Optimizing drug delivery in COPD: The role of inhaler devices. *Respir Med*. 2017;124:6-14. doi:10.1016/j.rmed.2017.01.006.
17. Daniher DI, Zhu J. Dry powder platform for pulmonary drug delivery. *Particuology*. 2008;6(4):225-238. doi:10.1016/j.partic.2008.04.004.
18. Chrystyn H. Closer to an Ideal Inhaler with the Easyhaler: AnInnovative Dry Powder Inhaler. *Clin Drug Investig*. 2006;26(4):1-10. http://www.ingentaconnect.com/content/adis/cdi/2006/00000026/00000004/art00001.
19. Yang MY, Chan JGY, Chan HK. *Pulmonary Drug Delivery by Powder Aerosols*. Vol 193. Elsevier B.V.; 2014. doi:10.1016/j.jconrel.2014.04.055.
20. Hoppentocht M, Hagedoorn P, Frijlink HW, de Boer AH. Technological and practical challenges of dry powder inhalers and formulations. *Adv Drug Deliv Rev*. 2014;75:18-31. doi:10.1016/j.addr.2014.04.004.
21. TwinCaps®. http://www.hovione.com/products-and-services/contract-manufacturing-services/drug-product/inhalation-drug-delivery-device-0. Accessed August 13, 2018.
22. Prime D. Review of dry powder inhalers. *Adv Drug Deliv Rev*. 1997;26(1):51-58. doi:10.1016/S0169-409X(97)00510-3.
23. De Boer AH, Le Brun PPH, Van der Woude HG, Hagedoorn P, Heijerman HGM, Frijlink HW. Dry powder inhalation of antibiotics in cystic fibrosis therapy, part 1: Development of a powder formulation with colistin sulfate for a special test inhaler with an air classifier as de-agglomeration principle. *Eur J Pharm Biopharm*. 2002;54(1):17-24. doi:10.1016/S0939-6411(02)00043-7.
24. Maa Y-F, Nguyen P-A, Sweeney T, Shire SJ, Hsu CC. Protein Inhalation Powders: Spray Drying vs Spray Freeze Drying. *Pharm Res*. 1999;Vol. 16(2):249-254.
25. Chow AHL, Tong HHY, Chattopadhyay P, Shekunov BY. Particle engineering for pulmonary drug delivery. *Pharm Res*. 2007;24(3):411-437. doi:10.1007/s11095-006-9174-3.
26. Telko MJ, Dsc AJH. Dry Powder Inhaler Formulation. 2005:1209-1227.
27. Pinto JT, Radivojev S, Zellnitz S, Roblegg E, Paudel A. How does secondary processing affect the physicochemical properties of inhalable salbutamol sulphate particles? A temporal investigation. *Int J Pharm*. 2017;528(1-2):416-428. doi:10.1016/j.ijpharm.2017.06.027.
28. Shur J, Pitchayajittipong C, Rogueda P, Price R. Effect of processing history on the surface interfacial properties of budesonide in carrier-based dry-powder inhalers. *Ther Deliv*. 2013;4(8):925-937. doi:10.4155/tde.13.69.
29. Hickey AJ. Complexity in Pharmaceutical Powders for Inhalation: A perspective. *KONA Powder Part J*. 2018;(April):1-11. doi:10.14356/kona.2018007.

30. Mangal S, Meiser F, Tan G, Gengenbach T, Morton DAV, Larson I. Applying surface energy derived cohesive-adhesive balance model in predicting the mixing, flow and compaction behaviour of interactive mixtures. *Eur J Pharm Biopharm*. 2016;104:110-116. doi:10.1016/j.ejpb.2016.04.021.
31. Kaialy W, Nokhodchi A. Particle Engineering for Improved Pulmonary Drug Delivery Through Dry Powder Inhalers. In: Nokhodchi A, Martin GP, eds. *Pulmonary Drug Delivery: Advances and Challenges*. 1st ed. John Wiley & Sons, Inc.; 2015:171-197.
32. Wu X, Li X, Mansour HM. Surface Analytical Techniques in Solid-State Particle Characterization for Predicting Performance in Dr y Powder Inhalers. *Powder Technol*. 2010;28(28):3-19. doi:https://doi.org/10.14356/kona.2010005.
33. Yu L. Amorphous pharmaceutical solids: Preparation, characterization and stabilization. *Adv Drug Deliv Rev*. 2001;48(1):27-42. doi:10.1016/S0169-409X(01)00098-9.
34. Depasquale R, Lee SL, Saluja B, Shur J, Price R. The Influence of Secondary Processing on the Structural Relaxation Dynamics of Fluticasone Propionate. *AAPS PharmSciTech*. 2015;16(3):589-600. doi:10.1208/s12249-014-0222-8.
35. Feeley JC, York P, Sumby BS, Dicks H. Determination of surface properties and flow characteristics of salbutamol sulphate, before and after micronisation. *Int J Pharm*. 1998;172(1-2):89-96. doi:10.1016/S0378-5173(98)00179-3.
36. Buckton G. Assessment of disorder in crystalline powders - a review of analytical techniques and their application. *Int J Pharm*. 1999;179(2):141-158. doi:10.1016/S0378-5173(98)00335-4.
37. Kulvanich P, Stewart PJ. The effect of particle size and concentration on the adhesive characteristics of a model drug-carrier interactive system. *J Pharm Pharmacol*. 1987;39(9):673-678. doi:10.1111/j.2042-7158.1987.tb06968.x.
38. Zeng XM, Martin GP, Marriott C. *Particulate Interactions in Dry Powder Formulations for Inhalation*. London; 2003. doi:10.1017/CBO9781107415324.004.
39. Dickhoff BHJ, Ellison MJH, De Boer AH, Frijlink HW. The effect of budesonide particle mass on drug particle detachment from carrier crystals in adhesive mixtures during inhalation. *Eur J Pharm Biopharm*. 2002;54(2):245-248. doi:10.1016/S0939-6411(02)00082-6.
40. Peng T, Lin S, Niu B, et al. Influence of physical properties of carrier on the performance of dry powder inhalers. *Acta Pharm Sin B*. 2016;6(4):308-318. doi:10.1016/j.apsb.2016.03.011.
41. Starch MCC, Inhalation L. Particle size measurement of lactose for dry powder inhalers.
42. Gottschalk N, Reuter LS, Zindler S, Föste H, Augustin W, Scholl S. Determination of cleaning mechanisms by measuring particle size distributions. *Food Bioprod Process*. 2018:1-9. doi:10.1016/j.fbp.2018.10.003.

43. Le VNP, Thi THH, Robins E, Flament MP. Dry Powder Inhalers: Study of the Parameters Influencing Adhesion and Dispersion of Fluticasone Propionate. *AAPS PharmSciTech*. 2012;13(2):477-484. doi:10.1208/s12249-012-9765-8.
44. Dickhoff BHJ, Boer AH De, Lambregts D, Frijlink HW. The effect of carrier surface treatment on drug particle detachment from crystalline carriers in adhesive mixtures for inhalation. 2006;327:17-25. doi:10.1016/j.ijpharm.2006.07.017.
45. Grasmeijer F, Lexmond AJ, Noort M Van Den, et al. New Mechanisms to Explain the Effects of Added Lactose Fines on the Dispersion Performance of Adhesive Mixtures for Inhalation. 2014;9(1):1-11. doi:10.1371/journal.pone.0087825.
46. Vehring R. Pharmaceutical particle engineering via spray drying. *Pharm Res*. 2008;25(5):999-1022. doi:10.1007/s11095-007-9475-1.
47. Fults KA, Miller IF, Hickey AJ. Effect of particle morphology on emitted dose of fatty acid-treated disodium cromoglycate powder aerosols. *Pharm Dev Technol*. 1997;2(1):67-79. doi:10.3109/10837459709022610.
48. De Boer AH, Chan HK, Price R. A critical view on lactose-based drug formulation and device studies for dry powder inhalation: Which are relevant and what interactions to expect? *Adv Drug Deliv Rev*. 2012;64(3):257-274. doi:10.1016/j.addr.2011.04.004.
49. Scanning electron microscope -SEM. https://www.zeiss.com/microscopy/int/products/scanning-electron-microscopes.html. Accessed February 7, 2018.
50. Scanning Electron Microscopes. https://www.nanoscience.com/technology/sem-technology/sem/. Accessed February 7, 2018.
51. Principle of SEM. https://en.wikipedia.org/wiki/Scanning_electron_microscope#/media/File:Schema_MEB_(en).svg. Accessed February 7, 2018.
52. Burnett DJ, Khoo J, Naderi M, Heng JYY, Wang GD, Thielmann F. Effect of Processing Route on the Surface Properties of Amorphous Indomethacin Measured by Inverse Gas Chromatography. *AAPS PharmSciTech*. 2012;13(4):1511-1517. doi:10.1208/s12249-012-9881-5.
53. Grimsey IM, Feeley JC, York P. Analysis of the surface energy of pharmaceutical powders by inverse gas chromatography. *J Pharm Sci*. 2002;91(2):571-583. doi:10.1002/jps.10060.
54. Lohrmann M, Kappl M, Butt HJ, Urbanetz NA, Lippold BC. Adhesion forces in interactive mixtures for dry powder inhalers - Evaluation of a new measuring method. *Eur J Pharm Biopharm*. 2007;67(2):579-586. doi:10.1016/j.ejpb.2007.02.011.
55. Podczeck F. Adhesion forces in interactive powder mixtures of a micronized drug and carrier particles of various particle size distributions. *J Adhes Sci Technol*.

1998;12(12):1323-1339. doi:10.1163/156856198X00461.

56. De Boer AH, Dickhoff BHJ, Hagedoorn P, et al. A critical evaluation of the relevant parameters for drug redispersion from adhesive mixtures during inhalation. *Int J Pharm*. 2005;294(1-2):173-184. doi:10.1016/j.ijpharm.2005.01.035.
57. Jones MD, Price R. The influence of fine excipient particles on the performance of carrier-based dry powder inhalation formulations. *Pharm Res*. 2006;23(8):1665-1674. doi:10.1007/s11095-006-9012-7.
58. Shah U V., Karde V, Ghoroi C, Heng JYY. Influence of particle properties on powder bulk behaviour and processability. *Int J Pharm*. 2017;518(1-2):138-154. doi:10.1016/j.ijpharm.2016.12.045.
59. Young PM, Wood O, Ooi J, Traini D. The influence of drug loading on formulation structure and aerosol performance in carrier based dry powder inhalers. *Int J Pharm*. 2011;416(1):129-135. doi:10.1016/j.ijpharm.2011.06.020.
60. Hickey AJ, Mansour HM, Telko MJ, et al. Physical characterization of component particles included in dry powder inhalers. I. Strategy review and static characteristics. *J Pharm Sci*. 2007;96(5):1282-1301. doi:10.1002/jps.20916.
61. Buttini F, Colombo G, Kwok PCL, Wui WT. Aerodynamic Assessment for Inhalation Products: Fundamentals and Current Pharmacopoeial Methods. In: *Inhalation Drug Delivery: Techniques and Products*. ; 2013:91-119. doi:10.1002/9781118397145.ch6.
62. Copley Scientific. Quality Solutions for Inhaler Testing. 2012.
63. Pinto JT, Zellnitz S, Guidi T, Roblegg E, Paudel A. Assessment of dry powder inhaler carrier targeted design: A comparative case-study of diverse anomeric compositions and physical properties of lactose. *Mol Pharm*. 2018;15:2827-2839. doi:10.1021/acs.molpharmaceut.8b00333.
64. Bresciani E, Barata T, Fagundes TC, Adachi A, Terrin MM, Navarro MF. Resistencia compresiva y tensil diametral de los comentos ionómeros vítreos. *Rev mínima Interv en Odontol*. 2008;1(2):102-111.
65. Klaja J, Łykowska G, Przelaskowska A. Helium porosity measurements for rocks from unconventional reservoirs performed on crushed samples. *Nafta-Gaz*. 2015;71(11):856-863. doi:10.18668/NG2015.11.07.
66. Stranzinger S, Faulhammer E, Calzolari V, et al. The effect of material attributes and process parameters on the powder bed uniformity during a low-dose dosator capsule filling process. *Int J Pharm*. 2017;516(1-2):9-20. doi:10.1016/j.ijpharm.2016.11.010.
67. Guenette E, Barrett A, Kraus D, Brody R, Harding L, Magee G. Understanding the effect of lactose particle size on the properties of DPI formulations using experimental design. *Int J Pharm*. 2009;380(1-2):80-88. doi:10.1016/j.ijpharm.2009.07.002.
68. Ooi J, Traini D, Hoe S, Wong W, Young PM. Does carrier size matter? A fundamental

study of drug aerosolisation from carrier based dry powder inhalation systems. *Int J Pharm*. 2011;413(1-2):1-9. doi:10.1016/j.ijpharm.2011.04.002.

69. Kaialy W, Martin GP, Larhrib H, Ticehurst MD, Kolosionek E, Nokhodchi A. The influence of physical properties and morphology of crystallised lactose on delivery of salbutamol sulphate from dry powder inhalers. *Colloids Surfaces B Biointerfaces*. 2012;89(1):29-39. doi:10.1016/j.colsurfb.2011.08.019.
70. Zeng XM, Martin GP, Tee SK, Marriott C. The role of fine particle lactose on the dispersion and deaggregation of salbutamol sulphate in an air stream in vitro. *Int J Pharm*. 1998;176(1):99-110. doi:10.1016/S0378-5173(98)00300-7.
71. Shur J, Harris H, Jones MD, Kaerger JS, Price R. The role of fines in the modification of the fluidization and dispersion mechanism within dry powder inhaler formulations. *Pharm Res*. 2008;25(7):1631-1640. doi:10.1007/s11095-008-9538-y.
72. Sympatec. Wet Dispersion - Sympatec. https://www.sympatec.com/en/particle-measurement/glossary/wet-dispersion/. Accessed May 23, 2018.
73. Kendall K, Stainton C. Adhesion and aggregation of fine particles. *Powder Technol*. 2001;121(2-3):223-229. doi:10.1016/S0032-5910(01)00386-2.
74. Behara SRB, Kippax P, McIntosh MP, Morton DAV, Larson I, Stewart P. Structural influence of cohesive mixtures of salbutamol sulphate and lactose on aerosolisation and de-agglomeration behaviour under dynamic conditions. *Eur J Pharm Sci*. 2011;42(3):210-219. doi:10.1016/j.ejps.2010.11.008.
75. Watling CP, Elliott JA, Scruton C, Cameron RE. Surface modification of lactose inhalation blends by moisture. *Int J Pharm*. 2010;391(1-2):29-37. doi:10.1016/j.ijpharm.2010.02.011.
76. Tien N. *Particle-Particle Interaction in Dry Powder Blending: Applying Theoretical Concepts to Practical Systems*.; 2014. https://www.tipharma.com/fileadmin/user_upload/Theses/PDF/Nguyen_Tien_Thanh_D6-203.pdf.
77. Badawy SI, Lee TJ, Menning MM. Effect of drug substance particle size on the characteristics of granulation manufactured in a high-shear mixer. *AAPS PharmSciTech*. 2000;1(4):E33. doi:10.1208/pt010433.
78. Kaialy W, Alhalaweh A, Velaga SP, Nokhodchi A. Effect of carrier particle shape on dry powder inhaler performance. *Int J Pharm*. 2011;421(1):12-23. doi:10.1016/j.ijpharm.2011.09.010.
79. Santl M, ILIc I, Vrecer F, Baumgartner S. A compressibility and compactibility study of real tableting mixtures: The effect of granule particle size. *Acta Pharm*. 2012;62(3):325-340. doi:10.2478/v10007-012-0028-8.
80. Cordts E, Steckel H. Capabilities and limitations of using powder rheology and

permeability to predict dry powder inhaler performance. *Eur J Pharm Biopharm*. 2012;82(2):417-423. doi:10.1016/j.ejpb.2012.07.018.

81. Shalash AO, Khalafallah NM, Molokhia AM, Elsayed MMA. The Relationship Between the Permeability and the Performance of Carrier-Based Dry Powder Inhalation Mixtures: New Insights and Practical Guidance. *AAPS PharmSciTech*. 2017. doi:10.1208/s12249-017-0898-7.
82. Kou X, Wah L, Steckel H, Heng PWS. Physico-chemical aspects of lactose for inhalation. *Adv Drug Deliv Rev*. 2012;64(3):220-232. doi:10.1016/j.addr.2011.11.004.
83. Iida K, Hayakawa Y, Okamoto H, Danjo K, Leuenberger H. Evaluation of flow properties of dry powder inhalation of salbutamol sulfate with lactose carrier. *Chem Pharm Bull (Tokyo)*. 2001;49(10):1326-1330. doi:10.1248/cpb.49.1326.
84. Buttini F, Brambilla G, Copelli D, et al. Effect of Flow Rate on In Vitro Aerodynamic Performance of NEXThaler® in Comparison with Diskus® and Turbohaler® Dry Powder Inhalers. *J Aerosol Med Pulm Drug Deliv*. 2016;29(2):167-178. doi:10.1089/jamp.2015.1220.
85. Grasmeijer F, Grasmeijer N, Hagedoorn P, Frijlink H, Haaije de Boer A. Recent advances in the fundamental understanding of adhesive mixtures for inhalation. *Curr Pharm Des*. 2015;21(40):5900-5914. doi:10.2174/1381612821666151008124622.
86. Du P, Du J, Smyth HDC. Evaluation of Granulated Lactose as a Carrier for DPI Formulations 1: Effect of Granule Size. *AAPS PharmSciTech*. 2014;15(6):1417-1428. doi:10.1208/s12249-014-0166-z.
87. Kaialy W, Nokhodchi A. Antisolvent crystallisation is a potential technique to prepare engineered lactose with promising aerosolisation properties: Effect of saturation degree. *Int J Pharm*. 2012;437(1-2):57-69. doi:10.1016/j.ijpharm.2012.07.064.
88. Wong L, Pilpel N. The effect of particle shape on the mechanical properties of powders. *Int J Pharm*. 1990;59(2):145-154. doi:10.1016/j.jallcom.2016.09.168.